

Data-Driven Stochastic Robust Optimization: A General Computational Framework and Algorithm for Optimization under Uncertainty in the Big Data Era

Chao Ning, Fengqi You*

Robert Frederick Smith School of Chemical and Biomolecular Engineering, Cornell University,
Ithaca, New York 14853, USA

Abstract

A novel data-driven stochastic robust optimization (DDSRO) framework is proposed to systematically and automatically handle labeled multi-class uncertainty data in optimization problems. Uncertainty data in large datasets are often collected from various conditions, which are encoded by class labels. A group of Dirichlet process mixture models and maximum likelihood estimation are employed for uncertainty modeling. A DDSRO framework is further proposed based on the data-driven uncertainty model through a bi-level optimization structure. The outer optimization problem follows a two-stage stochastic programming approach to optimize the expected objective across different data classes; robust optimization is nested as the inner problem to ensure the robustness of the solution while maintaining computational tractability. A tailored column-and-constraint generation algorithm is further developed to solve the resulting multi-level optimization problem efficiently. By leveraging the label information, the proposed approach generates 85.2% more net present value on average than the state-of-the-art in data-driven adaptive robust optimization for a case study of process network planning.

Key words: big data, optimization under uncertainty, Bayesian model, labeled uncertainty data, process design and operations

*Corresponding author. Phone: (607) 255-1162; Fax: (607) 255-9166; E-mail: fengqi.you@cornell.edu

1. Introduction

Labeled multi-class data are ubiquitous in a variety of areas and disciplines, such as process monitoring [1], multimedia studies [2, 3], and supervised machine learning [4, 5]. For example, process data are labeled with the operating modes of chemical plants [6], and text documents are tagged with labels to indicate their topics [7]. Yearly chemical demand data are attached with the labels of different government policies enacted at the corresponding year. Government could encourage or discourage a certain industry by the means of subsidies and tax rates. Due to the massive amount of available uncertainty data (realizations of uncertain parameters) and dramatic progress in big data analytics [4], data-driven optimization under uncertainty emerges as a promising paradigm [8-13]. Most existing data-driven optimization methods are restricted to unlabeled uncertainty data. However, recent work has revealed the significance of the labeled uncertainty data in decision-making under uncertainty [14]. Discarding labels and applying the existing methods to labeled uncertainty data ignores information embedded in labels, possibly compromising results and leading to sub-optimal solutions. Consequently, new modeling frameworks and computational algorithms are required for handling labeled multi-class uncertainty data.

Optimization under uncertainty has attracted tremendous attention from both academia and industry [15-18]. Uncertain parameters, if not being accounted for, could render the solution of an optimization problem suboptimal or even infeasible [19]. To this end, a plethora of mathematical programming techniques, such as stochastic programming and robust optimization [20-22], have been proposed to support decision making under uncertainty. These techniques have their respective strengths and weaknesses, which lead to different application scopes [23-30]. Stochastic programming focuses on the expected performance of a solution by leveraging the scenarios of uncertainty realization and their probability distribution [31-33]. However, this approach requires accurate information on the probability distribution, and the resulting optimization problem could become computationally challenging as the number of scenarios increases [34-36]. Robust optimization provides an alternative paradigm that does not require accurate knowledge on probability distributions of uncertain parameters [37-40]. It has attracted considerable interest owing to the merit of feasibility guarantee and computational tractability [40]. Nevertheless, robust optimization does not take advantage of available probability distribution information, and its solution usually suffers from the conservatism issue [41]. The state-of-the-art approaches for

optimization under uncertainty leverage the synergy of different optimization methods to inherit their corresponding strengths and complement respective weaknesses [42-44]. However, these approaches do not couple or automate the two stages of data analysis and optimization under uncertainty. Therefore, the goal of this work is to propose a novel data-driven optimization framework that organically integrates labeled uncertainty data information with the state-of-the-art optimization approach.

1.1. Motivating example

In this subsection, a motivating example is presented to illustrate the characteristics of conventional optimization methods, and to demonstrate that leveraging label information in optimization problem is critical.

The deterministic formulation of the motivating example is shown in (1).

$$\begin{aligned}
 & \min_{x,y} 3x_1 + 5x_2 + 6x_3 + 6y_1 + 10y_2 + 12y_3 \\
 & \text{s.t. } x_1 + x_2 + x_3 \leq 200 \\
 & \quad x_1 + y_1 \geq u_1 \\
 & \quad x_2 + y_2 \geq u_2 \\
 & \quad x_3 + y_3 \geq u_3 \\
 & \quad x_i, y_i \geq 0, \quad i = 1, 2, 3
 \end{aligned} \tag{1}$$

where x_1, x_2, x_3, y_1, y_2 and y_3 are decision variables, u_1, u_2 and u_3 are parameters. In the deterministic optimization problem setup, u_1, u_2 and u_3 are assumed to be known exactly.

In practice, the parameters u_1, u_2 and u_3 are subject to uncertainty. In a data-driven optimization setting, what decision makers know about these uncertain parameters are their realizations, also known as uncertainty data. The scatter plot of labeled uncertainty data is shown in Figure 1, where the points represent uncertainty realizations of u_1, u_2 and u_3 . A total of 1,000 labeled uncertainty data points are used for uncertainty modeling in this motivating example. There are 4 labels within uncertainty data, which indicate that there are 4 data classes in total. Note that uncertainty data points from different data classes are indicated with disparate shapes in Figure 1. Moreover, uncertainty data in the same data class could exhibit complex characteristics, such as correlation, asymmetry and multimode.

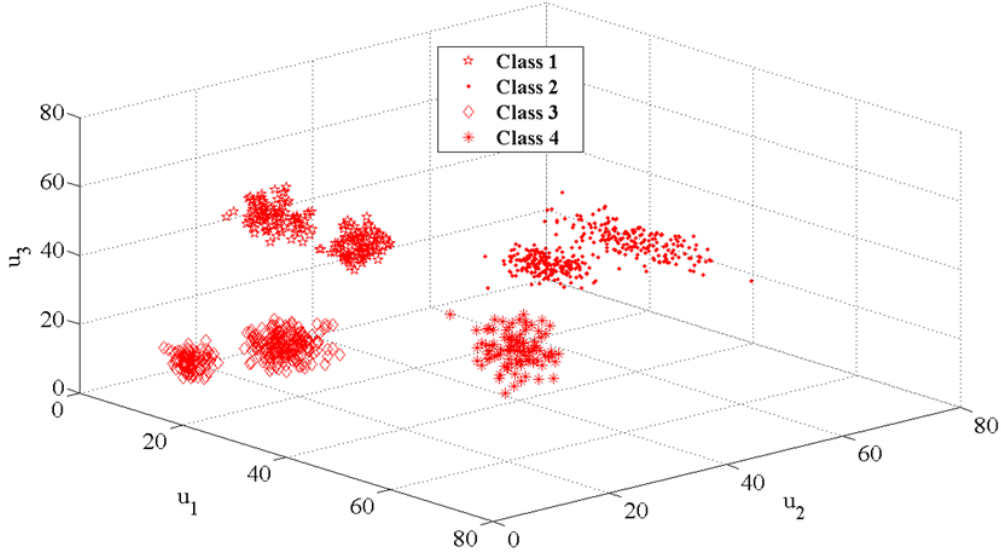


Figure 1. The scatter plot of uncertainty data in the motivating example.

One conventional way to hedging against uncertainty is the two-stage stochastic programming approach [20]. However, it is computationally challenging to fit a reasonable probability distribution to the uncertainty data points in Figure 1. If a scenario-based stochastic programming approach is applied to this problem, each data point in Figure 1 corresponds to a scenario. There are 1,000 scenarios in total, and the probability of each scenario is given as 0.001. The scenario-based two-stage stochastic programming model is shown as follows.

$$\begin{aligned}
& \min_{\mathbf{x}, \mathbf{y}_\omega} 3x_1 + 5x_2 + 6x_3 + \sum_{\omega \in \Theta} p_\omega \cdot [6y_{\omega,1} + 10y_{\omega,2} + 12y_{\omega,3}] \\
& \text{s.t. } x_1 + x_2 + x_3 \leq 200 \\
& \quad x_1 + y_{\omega,1} \geq u_{\omega,1} \quad \forall \omega \\
& \quad x_2 + y_{\omega,2} \geq u_{\omega,2} \quad \forall \omega \\
& \quad x_3 + y_{\omega,3} \geq u_{\omega,3} \quad \forall \omega \\
& \quad x_i, y_{\omega,i} \geq 0, \quad \forall \omega, i = 1, 2, 3
\end{aligned} \tag{2}$$

where the notation Θ represents the set of scenarios, and ω is the scenario index. The probability of each scenario is p_ω . x_1 , x_2 and x_3 are the first-stage or “here-and-now” decision variables, $u_{\omega,1}$, $u_{\omega,2}$ and $u_{\omega,3}$ are the uncertainty realizations, and $y_{\omega,1}$, $y_{\omega,2}$ and $y_{\omega,3}$ are the second-stage or “wait-and-see” decision variables corresponding to scenario ω . Note that the “here-and-now” decisions are made prior to the resolution of uncertainties, whereas “wait-and-see” decisions could be made

after the uncertainties are revealed. To speed up the solution, the resulting two-stage stochastic programming problem is solved using the multi-cut Benders decomposition algorithm [45].

An alternative way of optimization under uncertainty is the two-stage adaptive robust optimization (ARO) method [40]. The two-stage ARO model is shown as follows.

$$\begin{aligned}
& \min_{\mathbf{x}} 3x_1 + 5x_2 + 6x_3 + \max_{\mathbf{u} \in U} \min_{\mathbf{y}} 6y_1 + 10y_2 + 12y_3 \\
& \text{s.t. } x_1 + x_2 + x_3 \leq 200 \\
& \quad x_1 + y_1 \geq u_1 \\
& \quad x_2 + y_2 \geq u_2 \\
& \quad x_3 + y_3 \geq u_3 \\
& \quad U = \{\mathbf{u} \mid u_i^L \leq u_i \leq u_i^U, i = 1, 2, 3\} \\
& \quad x_i, y_i \geq 0, i = 1, 2, 3
\end{aligned} \tag{3}$$

where u_i^L and u_i^U are the lower and upper bound of uncertain parameter u_i , respectively. These two parameters can be readily derived from the uncertainty data in Figure 1.

The numerical results are shown in Table 1. In the deterministic optimization method, the uncertain parameters are set to be their mean values of the uncertainty data. Although the deterministic approach achieves a low objective value in the minimization problem, its optimal solution could become infeasible when the parameters u_1 , u_2 and u_3 are subject to uncertainty. The two-stage stochastic programming approach focuses on the expected objective value, while the two-stage ARO method aims to minimize the worst-case objective value. Therefore, the objective value of the two-stage stochastic programming approach is lower than that of the two-stage ARO method. Compared with the two-stage stochastic programming approach, the proposed DDSRO approach is much more computationally efficient.

A large amount of uncertainty data means more information that could be leveraged. Nevertheless, the two-stage stochastic programming problem could become computationally intractable as the number of uncertainty data increases. Moreover, the stochastic programming approach could not well capture uncertainty data if an inaccurate probability distribution is used to fit the data, thereby resulting in poor-quality solutions. Consequently, it might not be suitable to apply the conventional two-stage stochastic programming approach to the optimization problem where large amounts of uncertainty data are available. Despite its computational efficiency, the conventional two-stage ARO method only extracts coarse-grained uncertainty information on the

bounds of uncertain parameters. Huge waste of uncertainty information makes the conventional ARO method unsuitable for the data-driven optimization setting either.

The data-driven adaptive nested robust optimization (DDANRO) framework was recently proposed to overcome the drawback of the conventional ARO method [9]. The DDANRO model of this motivating example is given by

$$\begin{aligned}
& \min_{\mathbf{x}} 3x_1 + 5x_2 + 6x_3 + \max_{i \in \{1, \dots, m\}} \max_{\mathbf{u} \in U_i} \min_{\mathbf{y}} 6y_1 + 10y_2 + 12y_3 \\
& \text{s.t. } x_1 + x_2 + x_3 \leq 200 \\
& \quad x_1 + y_1 \geq u_1 \\
& \quad x_2 + y_2 \geq u_2 \\
& \quad x_3 + y_3 \geq u_3 \\
& \quad x_i, y_i \geq 0, \quad i = 1, 2, 3 \\
& \quad U_i = \left\{ \mathbf{u} \mid \mathbf{u} = \boldsymbol{\mu}_i + \kappa_i \boldsymbol{\Psi}_i^{1/2} \Lambda_i \mathbf{z}, \|\mathbf{z}\|_{\infty} \leq 1, \|\mathbf{z}\|_1 \leq \Delta_i \right\}
\end{aligned} \tag{4}$$

where U_i is the basic uncertainty set, $\boldsymbol{\mu}_i$, κ_i , $\boldsymbol{\Psi}_i$, and Λ_i are the parameters derived from uncertainty data. Δ_i is the uncertainty budget, and m represents the total number of the basic uncertainty sets.

Nevertheless, one limitation of the DDANRO method is that it does not leverage the label information in Figure 1 to infer the occurrence probability of each data class. This information derived from labels should inform the decision-making process. It motivates us to propose a data-driven stochastic robust optimization (DDSRO) framework as an extension of the DDANRO method for the labeled multi-class uncertainty data.

The DDSRO model formulation is given in (5). More details of the proposed DDSRO framework are provided in Section 2.

$$\begin{aligned}
& \min_{\mathbf{x}} 3x_1 + 5x_2 + 6x_3 + \mathbb{E}_{s \in \Xi} \left[\max_{\mathbf{u} \in U_s} \min_{\mathbf{y}} 6y_1 + 10y_2 + 12y_3 \right] \\
& \text{s.t. } x_1 + x_2 + x_3 \leq 200 \\
& \quad x_1 + y_1 \geq u_1 \\
& \quad x_2 + y_2 \geq u_2 \\
& \quad x_3 + y_3 \geq u_3 \\
& \quad x_i, y_i \geq 0, \quad i = 1, 2, 3
\end{aligned} \tag{5}$$

where the notation Ξ represents the set of data classes, and s is the corresponding element. The data-driven uncertainty set U_s for data class s is defined in (13).

Following the proposed data-driven uncertainty modeling framework in Section 2, the occurrence probabilities of different data classes are inferred from the label information embedded

within uncertainty data. The computational results show that the probabilities of data classes 1 - 4 are 0.2, 0.4, 0.3 and 0.1, respectively. Moreover, the uncertainty modeling results also show that there are two components in the Dirichlet process mixture models for data class 1-3, while there is only one component for data class 4. The occurrence probabilities of different data classes are listed in Figure 2. The data-driven uncertainty sets with uncertainty budget $\Phi=1.8$ are also constructed for each data class, and are depicted using different colors in Figure 2. From Figure 2, we can see that the distributional features of uncertainty data are automatically captured by the proposed data-driven uncertainty model. For example, the uncertainty set for data class 2 accurately captures the bimodal feature in uncertainty data, and the correlations among uncertain parameters u_1 , u_2 and u_3 . The computational results of the DDANRO and DDSRO methods are presented in Table 1.

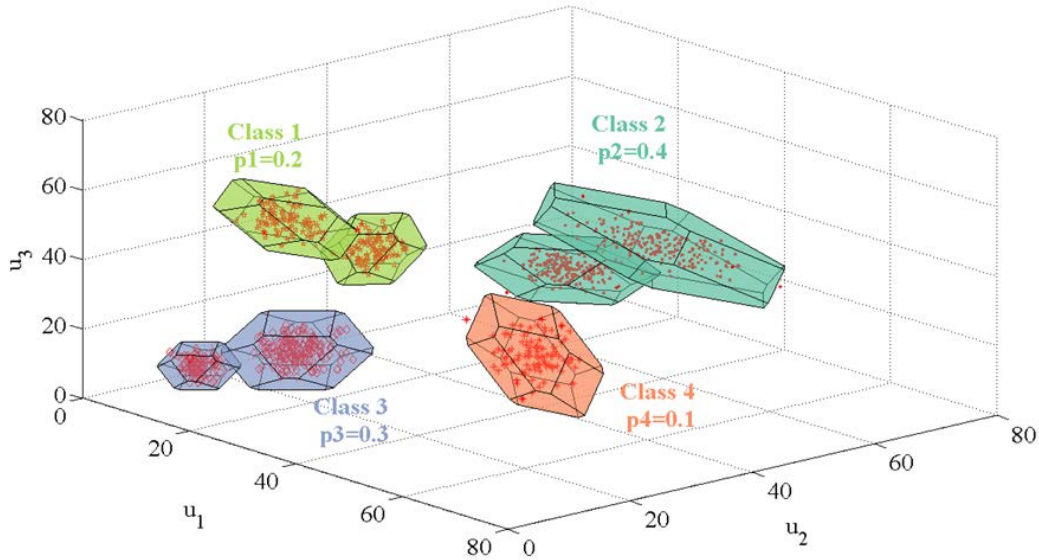


Figure 2. The data-driven uncertainty modeling results for the four data classes in the motivating example.

Table 1. Results of different optimization methods in the motivating example.

	Deterministic optimization	Two-stage stochastic programming	Two-stage ARO	DDANRO $\Delta=1.8^*$	DDSRO $\Phi=1.8^\#$
Min.obj.	455.3	646.4	964.0	944.6	795.4
Iterations	N/A	7	2	5	6
Total CPU (s)	0.1	477	1	9	12
Decision \mathbf{x}	$x_1 = 33.93$	$x_1 = 38.43$	$x_1 = 66.64$	$x_1 = 55.48$	$x_1 = 25.18$
	$x_2 = 29.55$	$x_2 = 27.55$	$x_2 = 62.49$	$x_2 = 52.56$	$x_2 = 33.62$
	$x_3 = 34.30$	$x_3 = 39.92$	$x_3 = 70.87$	$x_3 = 67.60$	$x_3 = 53.14$

* Δ is the data-driven uncertainty budget in the DDANRO approach.

Φ is the data-driven uncertainty budget in the DDSRO approach.

To compare the optimal solutions obtained from different approaches in an uncertain environment, we perform a simulation with randomly generated 500 uncertainty realizations. These 500 uncertainty realizations are generated in exactly the same way as we generate the original 1,000 labeled uncertainty data points. Specifically, these “testing” uncertainty realizations are from the same 4 data classes as in Figure 1, and the probability distribution for each data class is also the same as the one used to generate the uncertainty data points in Figure 1 such that the two datasets are independently and identically distributed. Although easier to obtain, the deterministic solution leads to infeasibility in 351 out of 500 (70.2%) uncertainty realizations. The simulation results of these three approaches are presented in Figure 3, in which the X-axis is the index of uncertainty realizations, and the Y-axis denotes the deterministic objective value (DOV). The expression for DOV is given in (6).

$$\text{DOV} = 3x_1 + 5x_2 + 6x_3 + 6y_1 + 10y_2 + 12y_3 \quad (6)$$

In Figure 3, the green dots represent the two-stage stochastic programming solutions. We can see that the two-stage stochastic programming approach generates a low DOV under most uncertainty realizations. However, its worst-case DOV is the largest one among all the three methods. The brown stars denote the DDANRO solutions. In contrast to the two-stage stochastic programming approach, the DDANRO method performs well under the worst-case uncertainty realization, and its DOV is insensitive to uncertainty. The purple rhombuses represent the DDSRO

solutions. Under most uncertainty realizations, the purple rhombuses are under the brown stars, which shows that the DDSRO approach performs better on average than the DDANRO method.

To quantify the performances of different approaches, the simulation results are summarized in Table 2. The DDSRO approach, by making full use of the label information, lowers the DOV of the state-of-the-art in data-driven adaptive robust optimization by 18.4%. It implies that the solution quality can be significant improved in optimization under uncertainty problems by leveraging labels.

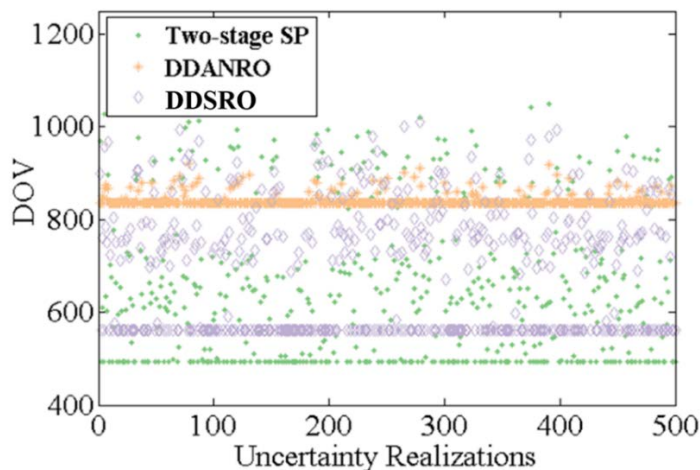


Figure 3. Simulation results for the two-stage stochastic programming approach, the DDANRO and DDSRO methods with randomly generated 500 uncertainty realizations in the motivating example. SP in the legend represents stochastic programming.

Table 2. Summary of the simulation results in the motivating example.

	Two-stage stochastic programming	Two-stage ARO	DDANRO	DDSRO
Expected DOV	643.3	937.7	840.8	686.2
Worst-case DOV	1,049.7	957.4	921.6	1,010.6
Standard deviation of DOV	156.7	1.2	14.5	130.6

1.2. Research challenges and novelties

There are a number of research challenges towards a general data-driven optimization framework for labeled multi-class uncertainty data. First, uncertainty data are often collected from a wide spectrum of conditions, which are indicated by categorical labels. For example, uncertain

power generation data of a solar farm are labeled with weather conditions, such as cloudy, sunny and rainy [46]. The occurrence probability of each weather condition is known in the data collection process, and typically embedded in the datasets. Moreover, the uncertainty data with the same label could exhibit very complicated distribution, which is impossible to fit using commonly known distributions. Therefore, a major research challenge is how to systematically and automatically handle labeled multi-class uncertainty data by leveraging the label information in the data-driven optimization framework. Second, we are confronted with the challenge of how to integrate different approaches for optimization under uncertainty in a holistic framework to leverage their respective advantages. The third challenge is to develop an efficient computational algorithm for the resulting large-scale multi-level optimization problem, which cannot be solved directly by any off-the-shelf optimization solvers.

This paper proposes a novel DDSRO framework that systematically and automatically handles labeled multi-class uncertainty data. In large datasets, uncertainty data are often attached with labels to indicate their data classes [4]. For the labeled multi-class uncertainty data, we propose a data-driven uncertainty modeling process that includes two parts, i.e. probability distribution estimation for different data classes, and uncertainty set construction for uncertainty. The probability distribution for data classes is learned from labeled uncertainty data through maximum likelihood estimation for the multinoulli distribution [5, 47]. It is worth noting that the amount of labeled uncertainty data should be large enough to ensure an accurate estimation of the probability distribution. To capture the nature of uncertainty data with different labels, a group of Dirichlet process mixture models are employed to model uncertainty with a variational inference algorithm [48, 49]. These two pieces of uncertainty information are incorporated into the DDSRO framework through a bi-level optimization structure. Two-stage stochastic programming is nested in the outer problem to optimize the expected objective over categorical data classes; robust optimization is nested as the inner problem to hedge against high-dimensional uncertainty and ensure computational tractability. Estimating a categorical distribution is much more computationally tractable than estimating a joint probability distribution of a high-dimensional uncertainty [5]. Therefore, the outer problem follows a two-stage stochastic programming structure to take advantage of the available probability information on data classes. Robust optimization, which uses an uncertainty set instead of accurate knowledge on probability distributions, is more suitable to be nested as the inner problem to tackle high-dimensional uncertainties. The DDSRO

problem is formulated as a multi-level mixed-integer linear program (MILP). We further develop a tailored column-and-constraint generation (C&CG) algorithm to efficiently solve the resulting multi-level MILP problem. To demonstrate the advantages of the proposed framework, two case studies on strategic planning of process networks under uncertainty are presented.

The major contributions of this paper are summarized as follows.

- A novel data-driven uncertainty modeling framework that systematically and automatically handles labeled multi-class uncertainty data;
- A general DDSRO framework that organically integrates uncertainty data information and a state-of-the-art approach for optimization under uncertainty;
- A tailored C&CG algorithm that efficiently solves the resulting multi-level MILP problems;
- A large-scale application on process network planning under uncertainty.

The rest of this paper is organized as follows. Section 2 presents the general DDSRO framework, which includes uncertainty modeling, optimization model and computational algorithm. It is followed by an application on process network planning under uncertainty in Section 3. A conclusion is drawn in Section 4.

2. Data-Driven Stochastic Robust Optimization Framework

In this section, we first provide a brief introduction to stochastic robust optimization. The proposed data-driven uncertainty model and the DDSRO framework are presented next. A decomposition-based solution algorithm is further developed to efficiently solve the resulting multi-level optimization problem.

2.1. Stochastic robust optimization

The stochastic robust optimization framework combines two-stage stochastic programming and ARO [43]. In this subsection, we first analyze the strengths and weaknesses of two-stage stochastic programming and two-stage ARO. They are then integrated in a novel form to leverage their corresponding advantages and complement respective shortcomings.

A general two-stage stochastic MILP in its compact form is given as follows [20].

$$\begin{aligned}
& \min_{\mathbf{x}} \mathbf{c}^T \mathbf{x} + \mathbb{E}_{\mathbf{u}} [Q(\mathbf{x}, \mathbf{u})] \\
& \text{s.t.} \quad \mathbf{Ax} \geq \mathbf{d} \\
& \quad \mathbf{x} \in R_+^{n_1} \times Z^{n_2}
\end{aligned} \tag{7}$$

The recourse function $Q(\mathbf{x}, \mathbf{u})$ is defined as follows.

$$\begin{aligned}
Q(\mathbf{x}, \mathbf{u}) &= \min_{\mathbf{y}} \mathbf{b}^T \mathbf{y} \\
& \text{s.t.} \quad \mathbf{Wy} \geq \mathbf{h} - \mathbf{T}\mathbf{x} - \mathbf{Mu} \\
& \quad \mathbf{y} \in R_+^{n_3}
\end{aligned} \tag{8}$$

where \mathbf{x} is first-stage decisions made “here-and-now” before the uncertainty \mathbf{u} is realized, while the second-stage decisions or recourse decisions \mathbf{y} are postponed in a “wait-and-see” manner after the uncertainties are revealed. \mathbf{x} can include both continuous and integer variables, while \mathbf{y} only includes continuous variables. The objective of (7) includes two parts: the first-stage objective $\mathbf{c}^T \mathbf{x}$ and the expectation of the second-stage objective $\mathbf{b}^T \mathbf{y}$. The constraints associated with the first-stage decisions are $\mathbf{Ax} \geq \mathbf{d}$, $\mathbf{x} \in R_+^{n_1} \times Z^{n_2}$, and the constraints of the second-stage decisions are $\mathbf{Wy} \geq \mathbf{h} - \mathbf{T}\mathbf{x} - \mathbf{Mu}$, $\mathbf{y} \in R_+^{n_3}$.

Two-stage stochastic programming makes full use of probability distribution information, and aims to find a solution that performs well on average under all scenarios. However, an accurate joint probability distribution of high-dimensional uncertainty \mathbf{u} is required to calculate the expectation term in (7). Besides, the resulting two-stage stochastic programming problem could become computationally challenging as the number of scenarios increases [35].

Another popular approach for optimization under uncertainty is ARO, which hedges against the worst-case uncertainty realization within an uncertainty set. A general two-stage ARO problem in its compact form is given as follows [50, 51].

$$\begin{aligned}
& \min_{\mathbf{x}} \mathbf{c}^T \mathbf{x} + \max_{\mathbf{u} \in U} \min_{\mathbf{y} \in \Omega(\mathbf{x}, \mathbf{u})} \mathbf{b}^T \mathbf{y} \\
& \text{s.t.} \quad \mathbf{Ax} \geq \mathbf{d}, \quad \mathbf{x} \in R_+^{n_1} \times Z^{n_2} \\
& \quad \Omega(\mathbf{x}, \mathbf{u}) = \{ \mathbf{y} \in R_+^{n_3} : \mathbf{Wy} \geq \mathbf{h} - \mathbf{T}\mathbf{x} - \mathbf{Mu} \}
\end{aligned} \tag{9}$$

where \mathbf{x} is the vector of first-stage decision variables, and \mathbf{y} represents the vector of second-stage decisions. Note that \mathbf{x} includes both continuous and integer variables, and \mathbf{y} is the vector of continuous recourse variables. The first-stage decisions are made “here-and-now” prior to the resolution of uncertainty \mathbf{u} , and the second-stage decisions are adjustable to uncertainty realizations in a “wait-and-see” mode. U is an uncertainty set that characterizes the region in which

uncertainty realization resides. Note that the two-stage ARO problem in (9) is a tri-level optimization problem.

Existing ARO methods typically assume the uncertainty set U is given and known a priori, rather than constructing it directly from uncertainty data [9]. Robust optimization does not leverage available probability distribution information. Moreover, existing ARO methods handle the uncertainty realizations as a whole, because the inner maximization problem over \mathbf{u} is not capable to differentiate the uncertainty data with different labels and handle them separately. Consequently, the resulting solution can be overly conservative.

The stochastic robust optimization framework was recently proposed to organically integrate the two-stage stochastic programming approach with the ARO method. A general form of the stochastic robust MILP is given by [43],

$$\begin{aligned}
& \min_{\mathbf{x}} \mathbf{c}^T \mathbf{x} + \mathbb{E}_{\sigma \in \Pi} [\bar{C}_\sigma(\mathbf{x})] \\
& \text{s.t.} \quad \mathbf{Ax} \geq \mathbf{d} \\
& \quad \mathbf{x} \in R_+^{n_1} \times Z^{n_2} \\
& \left. \begin{aligned}
& \bar{C}_\sigma(\mathbf{x}) = \max_{\mathbf{u} \in U_\sigma} \min_{\mathbf{y}_\sigma} \mathbf{b}^T \mathbf{y}_\sigma \\
& \text{s.t.} \quad \mathbf{Wy}_\sigma \geq \mathbf{h} - \mathbf{T}\mathbf{x} - \mathbf{Mu} \\
& \quad \mathbf{y}_\sigma \in R_+^{n_3}
\end{aligned} \right\}, \forall \sigma \in \Pi
\end{aligned} \tag{10}$$

where σ is an uncertain scenario that influences the uncertainty set, and Π is a set of the scenarios. Two-stage stochastic programming approach is nested in the outer problem to optimize the expectation of objectives for different scenarios, and robust optimization is nested inside to hedge against the worst-case uncertainty realization. Stochastic robust optimization is capable of handling different types of uncertainties in a holistic framework.

The stochastic robust optimization method typically assumes the uncertainty probability distributions and uncertainty sets are given and known a priori, rather than connecting them directly with the uncertainty data. This assumption limits its application to the cases that uncertainty data are available, since the predefined probability distribution and manually constructed uncertainty sets might not capture fine-grained information from the available uncertainty data. Thus, we propose a novel data-driven uncertainty modeling framework for stochastic robust optimization with labeled multi-class uncertainty data to fill this knowledge gap.

2.2. Data-driven uncertainty modeling

In this subsection, we propose a data-driven uncertainty modeling framework that includes two parts, i.e. probability distribution estimation for different data classes, and uncertainty set construction from uncertainty data of the same data class. For the first part, the probability distribution for data classes is learned from the label information in mixed uncertainty data through maximum likelihood estimation. For the second part, a group of Dirichlet process mixture models is employed to construct uncertainty sets with a variational inference algorithm [49].

We consider the multi-class uncertainty data with labels $\{\mathbf{u}^{(i)}, c^{(i)}\}_{i=1}^L$, where $\mathbf{u}^{(i)}$ is i th uncertainty data point, $c^{(i)}$ is its corresponding label, and L is the total number of uncertainty data. Although the labeled uncertainty data is of practical relevance [4, 14], existing literature on data-driven optimization under uncertainty are restricted to unlabeled uncertainty data $\{\mathbf{u}^{(i)}\}_{i=1}^L$ [9, 13].

The uncertainty information on the probability of different data classes can be extracted from labeled uncertainty data by leveraging their label information. The occurrence probabilities of data classes are modeled with a multinoulli distribution. The probability of each data class can be calculated through maximum likelihood estimation, as shown in (11) [5, 47].

$$p_s = \frac{\sum_i \mathbb{I}(c^{(i)} = s)}{L} \quad (11)$$

where p_s represents the occurrence probability of data class s , $c^{(i)}$ is the label associated with the i th uncertainty data point, $c^{(i)=s}$ indicates that the i th uncertainty data point is from data class s , and the indicator function is defined as follows.

$$\mathbb{I}(c^{(i)} = s) = \begin{cases} 1 & \text{if } c^{(i)} = s \\ 0 & \text{else} \end{cases} \quad (12)$$

As will be shown in the next subsection, the extracted probability distribution information for different data classes is incorporated into the two-stage stochastic programming framework nested as the outer optimization problem of DDSRO.

The second part of the uncertainty modeling is the construction of data-driven uncertainty sets for uncertainty data in the same data class. The information on uncertainty sets is incorporated into the robust optimization nested as the inner optimization problem of DDSRO. To handle the labeled multi-class uncertainty data, a group of Dirichlet process mixture models is employed, and

uncertainty data with the same label are modeled using one separate Dirichlet process mixture model [49]. The details of Dirichlet process mixture model are given in Appendix A.

Based on the extracted information from Dirichlet process mixture model, we construct a data-driven uncertainty set for data class s using both l_1 and l_∞ norms in (13) and (14) [9].

$$U_s = \bigcup_{i: \gamma_{s,i} \geq \gamma^*} U_{s,i} = U_{s,1} \bigcup U_{s,2} \cdots \bigcup U_{s,m(s)} \quad (13)$$

$$U_{s,i} = \left\{ \mathbf{u} \mid \mathbf{u} = \boldsymbol{\mu}_{s,i} + \kappa_{s,i} \boldsymbol{\Psi}_{s,i}^{1/2} \Lambda_{s,i} \mathbf{z}, \|\mathbf{z}\|_\infty \leq 1, \|\mathbf{z}\|_1 \leq \Phi_{s,i} \right\} \quad (14)$$

where U_s is the data-driven uncertainty set for data class s , $U_{s,i}$ is the basic uncertainty set corresponding to the i th component for data class s , $\Lambda_{s,i}$ is a scaling factor, $\gamma_{s,i}$ is the weight of the

i th component for data class s , $\gamma_{s,i} = \frac{\tau_{s,i}}{\tau_{s,i} + \nu_{s,i}} \prod_{j=1}^{i-1} \frac{\nu_{s,j}}{\tau_{s,j} + \nu_{s,j}}$ and $\gamma_{s,M} = 1 - \sum_{i=1}^{M-1} \gamma_{s,i}$. The weight $\gamma_{s,i}$

indicates the probability of the corresponding component. γ^* is a threshold value. $m(s)$ is the total

number of components for data class s . $\kappa_{s,i} = \sqrt{\frac{\lambda_{s,i} + 1}{\lambda_{s,i} (\omega_{s,i} + 1 - \dim(\mathbf{u}))}}$ [48], $\tau_{s,i}$, $\nu_{s,i}$, $\boldsymbol{\mu}_{s,i}$, $\lambda_{s,i}$, $\omega_{s,i}$, $\boldsymbol{\Psi}_{s,i}$

are the inference results of the i th component learned from uncertainty data of data class s , and $\Phi_{s,i}$ is its uncertainty budget. It is worth noting that the number of basic uncertainty sets $m(s)$ for each data class can be different.

The proposed data-driven uncertainty modeling approach combines probability distribution estimation for different data classes with uncertainty set construction for the high-dimensional uncertainty. A novel DDSRO approach is further proposed by organically integrating this data-driven uncertainty model with the stochastic robust optimization framework.

2.3. Data-driven stochastic robust optimization model

Based on the uncertainty information, DDSRO framework is proposed to organically integrate uncertainty data information with the stochastic robust optimization framework, as shown in (15).

$$\begin{aligned}
& \min_{\mathbf{x}} \mathbf{c}^T \mathbf{x} + \mathbb{E}_{s \in \Xi} \left[\max_{\mathbf{u} \in U_{s,1} \cup U_{s,2} \dots \cup U_{s,m(s)}} \min_{\mathbf{y}_s \in \Omega(\mathbf{x}, \mathbf{u})} \mathbf{b}^T \mathbf{y}_s \right] \\
& \text{s.t. } \mathbf{Ax} \geq \mathbf{d}, \quad \mathbf{x} \in R_+^{n_1} \times Z^{n_2} \\
& U_{s,i} = \left\{ \mathbf{u} \mid \mathbf{u} = \boldsymbol{\mu}_{s,i} + \kappa_{s,i} \boldsymbol{\Psi}_{s,i}^{1/2} \boldsymbol{\Lambda}_{s,i} \mathbf{z}, \|\mathbf{z}\|_\infty \leq 1, \|\mathbf{z}\|_1 \leq \Phi_{s,i} \right\} \\
& \Omega(\mathbf{x}, \mathbf{u}) = \left\{ \mathbf{y}_s \in R_+^{n_3} : \mathbf{W}\mathbf{y}_s \geq \mathbf{h} - \mathbf{T}\mathbf{x} - \mathbf{M}\mathbf{u} \right\}
\end{aligned} \tag{15}$$

where $\Xi = \{1, 2, \dots, C\}$ is the set of data classes, C is the total number of data classes, $m(s)$ is the total number of mixture components for data class s . Each data class corresponds to a scenario in the two-stage stochastic program nested outside the DDSRO framework. Therefore, a data class corresponds to a scenario in the DDSRO framework. It is worth noting that the DDSRO problem in (15) is a multi-level MILP that involves mixed-integer first-stage decisions, and continuous recourse decisions.

In the DDSRO framework, the outer optimization problem follows a two-stage stochastic programming structure, and robust optimization is nested as the inner optimization problem to handle high-dimensional uncertainty \mathbf{u} . DDSRO aims to find a solution that performs well on average across all data classes by making full use of their occurrence probabilities. Instead of treating all the uncertainty data as a whole, we explicitly account for uncertainty data with different labels in the DDSRO framework. Stochastic robust optimization structure is employed because it is more suitable to handle different types of uncertainties in a holistic framework. Note that DDSRO is a general framework for data-driven optimization under uncertainty, while existing stochastic robust optimization methods assume uncertainty information is given *a priori* rather than learning it from uncertainty data.

There are two reasons that two-stage stochastic programming is nested as the outer optimization problem while robust optimization is nested as the inner optimization problem. First, the proposed DDSRO framework aims to balance all data classes instead of focusing only on the worst-case data class, and it also ensures the robustness of the solution. Second, estimating the probability distribution for data classes accurately is much more computationally tractable than for the high-dimensional continuous uncertainty [5]. Consequently, it is better to employ uncertainty set to characterize high-dimensional uncertain parameters in the inner optimization problem. On the other hand, stochastic programming is more suitable as the outer optimization problem to leverage the probability information of data classes.

Note that the proposed data-driven uncertainty set for each data class in (13) is a union of several basic uncertainty sets. Therefore, we reformulate the DDSRO model in (15) into (16), as given below.

$$\begin{aligned}
& \min_{\mathbf{x}} \mathbf{c}^T \mathbf{x} + \mathbb{E}_{s \in \Xi} \left[\max_{i \in \{1, \dots, m(s)\}} \max_{\mathbf{u} \in U_{s,i}} \min_{\mathbf{y}_s \in \Omega(\mathbf{x}, \mathbf{u})} \mathbf{b}^T \mathbf{y}_s \right] \\
& \text{s.t. } \mathbf{Ax} \geq \mathbf{d}, \quad \mathbf{x} \in R_+^{n_1} \times Z^{n_2} \\
& \quad U_{s,i} = \left\{ \mathbf{u} \mid \mathbf{u} = \boldsymbol{\mu}_{s,i} + \kappa_{s,i} \boldsymbol{\Psi}_{s,i}^{1/2} \boldsymbol{\Lambda}_{s,i} \mathbf{z}, \|\mathbf{z}\|_\infty \leq 1, \|\mathbf{z}\|_1 \leq \Phi_{s,i} \right\} \\
& \quad \Omega(\mathbf{x}, \mathbf{u}) = \left\{ \mathbf{y}_s \in R_+^{n_3} : \mathbf{W}\mathbf{y}_s \geq \mathbf{h} - \mathbf{T}\mathbf{x} - \mathbf{M}\mathbf{u} \right\}
\end{aligned} \tag{16}$$

Due to the finite number of data classes, the model in (16) is further reformulated with the occurrence probability for each data class as shown in (17).

$$\begin{aligned}
& \min_{\mathbf{x}} \mathbf{c}^T \mathbf{x} + \sum_{s \in \Xi} p_s \cdot \left(\max_{i \in \{1, \dots, m(s)\}} \max_{\mathbf{u} \in U_{s,i}} \min_{\mathbf{y}_s \in \Omega(\mathbf{x}, \mathbf{u})} \mathbf{b}^T \mathbf{y}_s \right) \\
& \text{s.t. } \mathbf{Ax} \geq \mathbf{d}, \quad \mathbf{x} \in R_+^{n_1} \times Z^{n_2} \\
& \quad U_{s,i} = \left\{ \mathbf{u} \mid \mathbf{u} = \boldsymbol{\mu}_{s,i} + \kappa_{s,i} \boldsymbol{\Psi}_{s,i}^{1/2} \boldsymbol{\Lambda}_{s,i} \mathbf{z}, \|\mathbf{z}\|_\infty \leq 1, \|\mathbf{z}\|_1 \leq \Phi_{s,i} \right\} \\
& \quad \Omega(\mathbf{x}, \mathbf{u}) = \left\{ \mathbf{y}_s \in R_+^{n_3} : \mathbf{W}\mathbf{y}_s \geq \mathbf{h} - \mathbf{T}\mathbf{x} - \mathbf{M}\mathbf{u} \right\}
\end{aligned} \tag{17}$$

where p_s represents the occurrence probability of data class s , and can be calculated by (11). Note that the uncertainty information extracted from data, including data-driven uncertainty sets and probability distributions of data classes, is seamlessly integrated into the optimization model in (17).

The DDSRO model explicitly accounts for the label information within multi-class uncertainty data, and balances different data classes by using the weighted sum based on their occurrence probabilities. Robust optimization is nested as the inner optimization problem to handle high-dimensional uncertainty \mathbf{u} , thus providing a good balance between solution quality and computational tractability. Moreover, multiple basic uncertainty sets $U_{s,i}$ are unified to handle the data complexity (such as correlation, asymmetry and multimode), and this approach leads to the inner max-max optimization problem in (17). An overview of the proposed DDSRO framework for labeled multi-class uncertainty data is shown in Figure 4. Uncertainty data are depicted using circles with different colors to indicate its associated data class, and they are treated separately using a group of Dirichlet process mixture models. The probability distribution of data classes can be obtained from uncertainty data using eq. (11). As can be observed, the proposed framework,

which leverages the strengths of stochastic programming and robust optimization, unlocks the value of labeled multi-class uncertainty data.

The resulting DDSRO problem is a multi-level MILP problem. Due to the multi-level structure, it cannot be solved directly by any general-purpose optimization solvers. To this end, an efficient computational algorithm is further proposed in the next subsection to address this computational challenge.

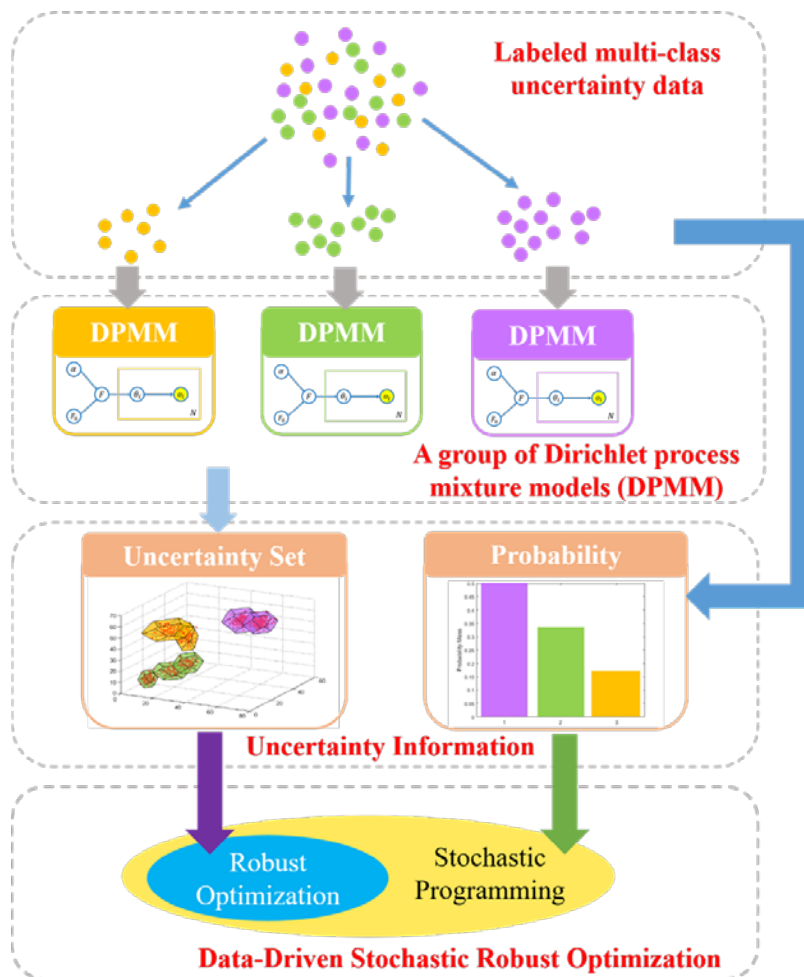


Figure 4. The proposed DDSRO framework that handles labeled multi-class uncertainty data.

2.4. The tailored column-and-constraint generation algorithm

In this section, we address computational challenge of solving the multi-level DDSRO problem by developing a decomposition-based solution algorithm. This algorithm is designed in the line of the C&CG algorithm [9, 51]. We first decompose the multi-level MILP shown in (17) into a master problem and many groups of sub-problems, where each group corresponds to a data

class. Moreover, there are a number of sub-problems in each group, and each sub-problem corresponds to a component in the Dirichlet process mixture model.

The proposed computational algorithm iteratively solves a sequence of master problem and sub-problems until the relative optimality gap reaches below the predefined tolerance ζ . The pseudocode of the algorithm is given in Figure 5, where C represents the total number of data classes. The algorithm is guaranteed to terminate within finite iterations due to the finite number of extreme points. The details of the proposed tailored C&CG algorithm, including the formulations of master problem (**MP**) and sub-problem (**SUP_{s,i}**), are given in Appendix B.

Algorithm. The proposed tailored C&CG algorithm

```

1:   Set  $LB \leftarrow -\infty$ ,  $UB \leftarrow +\infty$ ,  $k \leftarrow 0$ , and  $\zeta$ ;
2:   while  $\left| \frac{UB-LB}{UB} \right| > \zeta$  do
3:       Solve (MP) to obtain  $\mathbf{x}_{k+1}^*, \eta_{k+1}^*, \mathbf{y}_s^{1*}, \dots, \mathbf{y}_s^{k*}$ ;
4:       Update  $LB \leftarrow \mathbf{c}^T \mathbf{x}_{k+1}^* + \eta_{k+1}^*$ ;
5:       for  $s=1$  to  $C$  do
6:           for  $i=1$  to  $m(s)$  do
7:               Solve (SUPs,i) to obtain  $\mathbf{u}_{s,i}^{k+1}$  and  $Q_{s,i}(\mathbf{x}_{k+1}^*)$ ;
8:           end
9:            $i^* \leftarrow \arg \max_i Q_{s,i}(\mathbf{x}_{k+1}^*)$ ;
10:           $\mathbf{u}_s^{k+1} \leftarrow \mathbf{u}_{s,i^*}^{k+1}$  and  $Q_s(\mathbf{x}_{k+1}^*) \leftarrow Q_{s,i^*}(\mathbf{x}_{k+1}^*)$ ;
11:       end
12:       Update  $UB \leftarrow \min \left\{ UB, \mathbf{c}^T \mathbf{x}_{k+1}^* + \sum_{s=1}^C p_s \cdot Q_s(\mathbf{x}_{k+1}^*) \right\}$ ;
13:       Create second-stage variables  $\mathbf{y}_s^{k+1}$  and add cuts
            $\eta \geq \sum_s p_s (\mathbf{b}^T \mathbf{y}_s^{k+1})$  and  $\mathbf{T}\mathbf{x} + \mathbf{W}\mathbf{y}_s^{k+1} \geq \mathbf{h} - \mathbf{M}\mathbf{u}_s^{k+1}$  to (MP);
14:        $k \leftarrow k + 1$ ;
15:   end
16:   return  $UB$ ;

```

Figure 5. The pseudocode of the proposed computational algorithm.

2.5. Relationship with the existing data-driven adaptive nested robust optimization framework

In this subsection, we discuss the relationship between the DDSRO framework proposed in this work and the recently proposed DDANRO framework reported in our earlier publication [9].

The DDANRO framework in its general form has a four-level optimization structure, as given below.

$$\begin{aligned}
& \min_{\mathbf{x}} \mathbf{c}^T \mathbf{x} + \max_{i \in \{1, \dots, m\}} \max_{\mathbf{u} \in U_i} \min_{\mathbf{y} \in \Omega(\mathbf{x}, \mathbf{u})} \mathbf{b}^T \mathbf{y} \\
& \text{s.t. } \mathbf{A}\mathbf{x} \geq \mathbf{d}, \quad \mathbf{x} \in R_+^{n_1} \times Z^{n_2} \\
& U_i = \left\{ \mathbf{u} \mid \mathbf{u} = \boldsymbol{\mu}_i + \kappa_i \boldsymbol{\Psi}_i^{1/2} \boldsymbol{\Lambda}_i \mathbf{z}, \quad \|\mathbf{z}\|_\infty \leq 1, \|\mathbf{z}\|_1 \leq \Delta_i \right\} \\
& \Omega(\mathbf{x}, \mathbf{u}) = \left\{ \mathbf{y} \in R_+^{n_3} : \mathbf{W}\mathbf{y} \geq \mathbf{h} - \mathbf{T}\mathbf{x} - \mathbf{M}\mathbf{u} \right\}
\end{aligned} \tag{18}$$

It is worth noting that the DDSRO framework proposed in this paper could be considered as a generalization of the DDANRO framework, which handles uncertainty data homogeneously without considering the label information [9]. DDSRO greatly enhances the capabilities of DDANRO, and expands its application scope to more complex uncertainty data structures. There are some similarities between DDSRO and DDANRO. For example, they both employ data-driven uncertainty sets, and have multi-level optimization structures. Moreover, DDANRO can be considered as a special case of DDSRO when there is only one class of uncertainty data. Specifically, if there is only one data class, we can simplify the weighted sum in (17) as a single term, and drop index s in (17), such that the DDSRO model shown in (17) reduces to the DDANRO model in (18). Thus, the DDANRO framework is more appropriate to handle single-class or unlabeled uncertainty data, while the proposed DDSRO framework, on the other hand, is suitable for handling labeled multi-class uncertainty data systematically.

3. Application: Data-Driven Stochastic Robust Planning of Chemical Process Networks under Supply and Demand Uncertainties

The application of the proposed DDSRO framework to a multi-period process network planning problem is presented in this section. Large integrated chemical complexes consist of interconnected processes and various chemicals (see Figure 11 for an example) [52, 53]. These interconnections allow the chemical production to make the most of different processes [54, 55].

The chemicals in the process network include feedstocks, intermediates and final products. In the process network planning problem, purchase levels of feedstocks, sales of final products, capacity expansions, and production profiles of processes at each time period should be determined in order to maximize the net present value (NPV) during the entire planning horizon [56]. In the application, the supply of feedstocks and demand of products are subject to uncertainty.

3.1. Data-driven stochastic robust planning of process networks model

The DDSRO model for process network planning under uncertainty is formulated as follows. The objective is to maximize the NPV, which is given in (19). The constraints include capacity expansion constraints (20)-(21), budget constraints (22)-(23), production level constraint (24), mass balance constraint (25), supply and demand constraints (26)-(27), non-negativity constraints (28)-(29), and integrity constraint (30). A list of indices/sets, parameters and variables is given in Notation section, where all the parameters are in lower-case symbols, and all the variables are denoted in upper-case symbols.

The objective function is defined by (19).

$$\max_{QE_{it}, Y_{it}} - \sum_{i \in I} \sum_{t \in T} (c1_{it} \cdot QE_{it} + c2_{it} \cdot Y_{it}) + \mathbb{E}_{s \in \Xi} \left[\min_{du_{jt} \in U_s^{\text{dem}}, su_{jt} \in U_s^{\text{sup}}} \max_{P_{sjt}, Q_{sit}, SA_{sjt}, W_{sit}} \left(\sum_{j \in J} \sum_{t \in T} v_{jt} \cdot SA_{sjt} - \sum_{i \in I} \sum_{t \in T} c3_{it} \cdot W_{sit} - \sum_{j \in J} \sum_{t \in T} c4_{jt} \cdot P_{sjt} \right) \right] \quad (19)$$

where QE_{it} is a decision variable for capacity expansion of process i at period t , Y_{it} is a binary decision variable to determine on whether process i is expanded at period t , SA_{sjt} is the amount of chemical j sold to the market at period t for data class s , W_{sit} represents the operating level of process i at period t for data class s , and P_{sjt} is a decision variable on the amount of chemical j purchased at period t for data class s . $c1_{it}$, $c2_{it}$, $c3_{it}$ and $c4_{jt}$ are the coefficients associated with variable investment cost, fixed investment cost, operating cost and purchase cost, respectively. v_{jt} is the sale price of chemical j in time period t .

Constraint (20) specifies the lower and upper bounds of the capacity expansions. Specifically, if $Y_{it}=1$, i.e. process i is selected to be expanded at period t , the expanded capacity should be within the range $[qe_{it}^L, qe_{it}^U]$.

$$qe_{it}^L \cdot Y_{it} \leq QE_{it} \leq qe_{it}^U \cdot Y_{it}, \quad \forall i, t \quad (20)$$

Constraint (21) depicts the update of capacity of process i .

$$Q_{it} = Q_{it-1} + QE_{it}, \quad \forall i, t \quad (21)$$

where Q_{it} is a decision variable for total capacity of process i at period t .

Constraints (22) and (23) enforce the largest number of capacity expansions for process and investment budget, respectively.

$$\sum_t Y_{it} \leq ce_i, \quad \forall i \quad (22)$$

$$\sum_i (c1_{it} \cdot QE_{it} + c2_{it} \cdot Y_{it}) \leq cb_t, \quad \forall t \quad (23)$$

where ce_i is the largest possible expansion times of process i , and cb_t is the investment budget for period t .

Constraint (24) specifies that the production level of a process cannot exceed its total capacity.

$$W_{sit} \leq Q_{it}, \quad \forall s, i, t \quad (24)$$

Constraint (25) specifies the mass balance for chemicals.

$$P_{sjt} - \sum_i \kappa_{ij} \cdot W_{sit} - SA_{sjt} = 0, \quad \forall s, j, t \quad (25)$$

where κ_{ij} represents the mass balance coefficient of chemical j in process i .

Constraint (26) specifies that the purchase amount of a feedstock cannot exceed its available amount. The sale amount of a product and its market demand are specified in Constraint (27).

$$P_{sjt} \leq su_{jt}, \quad \forall s, j, t \quad (26)$$

$$SA_{sjt} \leq du_{jt}, \quad \forall s, j, t \quad (27)$$

where su_{jt} is the market availability and du_{jt} is the demand of chemical j in time period t .

Constraints (28)-(29) enforces the non-negativity of continuous decisions.

$$QE_{it} \geq 0, Q_{it} \geq 0 \quad \forall i, t \quad (28)$$

$$P_{sjt}, SA_{sjt}, W_{sit} \geq 0, \quad \forall s, j, t \quad (29)$$

Constraint (30) ensures that Y_{it} is a binary decision variable.

$$Y_{it} \in \{0, 1\}, \quad \forall i, t \quad (30)$$

Uncertainty information for demand and supply uncertainties is shown in (31)-(32).

$$U_s^{dem} = \bigcup_{k: \gamma_{s,k}^{dem} \geq \gamma^*} \left\{ \mathbf{d}\mathbf{u} \mid \mathbf{d}\mathbf{u} = \boldsymbol{\mu}_{s,k}^{dem} + \boldsymbol{\kappa}_{s,k}^{dem} \cdot \sqrt{\boldsymbol{\Psi}_{s,k}^{dem}} \cdot \boldsymbol{\Lambda}_{s,k}^{dem} \cdot \mathbf{z}, \|\mathbf{z}\|_{\infty} \leq 1, \|\mathbf{z}\|_1 \leq \Phi_{s,k}^{dem} \right\} \quad (31)$$

where $\boldsymbol{\mu}_{s,k}^{dem}$, $\boldsymbol{\kappa}_{s,k}^{dem}$, $\boldsymbol{\Psi}_{s,k}^{dem}$ are the inference results learned from uncertain product demand data using the Variational inference algorithm.

$$U_s^{\text{sup}} = \bigcup_{k: \gamma_{s,k}^{\text{sup}} \geq \gamma^*} \left\{ \mathbf{su} \mid \mathbf{su} = \boldsymbol{\mu}_{s,k}^{\text{sup}} + s_{s,k}^{\text{sup}} \cdot \sqrt{\boldsymbol{\Psi}_{s,k}^{\text{sup}}} \cdot \boldsymbol{\Lambda}_{s,k}^{\text{sup}} \cdot \mathbf{z}, \|\mathbf{z}\|_{\infty} \leq 1, \|\mathbf{z}\|_1 \leq \Phi_{s,k}^{\text{sup}} \right\} \quad (32)$$

where $\boldsymbol{\mu}_{s,k}^{\text{sup}}$, $\kappa_{s,k}^{\text{sup}}$, $\boldsymbol{\Psi}_{s,k}^{\text{sup}}$ are the inference results learned from uncertain supply data employing the Variational inference algorithm. The probabilities of different data classes are extracted using maximum likelihood estimation.

The resulting problem on strategic planning of process network under uncertainty is a multi-level MILP. The proposed computational algorithm is employed to efficiently solve the large-scale optimization problem. In the next two subsections, two case studies are presented to demonstrate the applicability and advantages of the proposed approach.

3.2. Case study 1

A small-scale case study is provided in this subsection. The process network, which is shown in Figure 6, consists of 5 chemicals, 3 processes, 3 suppliers and 2 markets [53]. In Figure 6, chemicals A-C represent raw materials, which can be either purchased from certain suppliers or produced by processes. For example, Chemical C can be either manufactured by Process 3 or purchased from a supplier. Chemicals D and E are final products, which are sold to the markets. In this case study, we consider 10 time periods over the 20-year planning horizon, and the duration of each time period is 2 years. It is assumed that processes do not have initial capacities, and they can be installed at the beginning of time period 1.

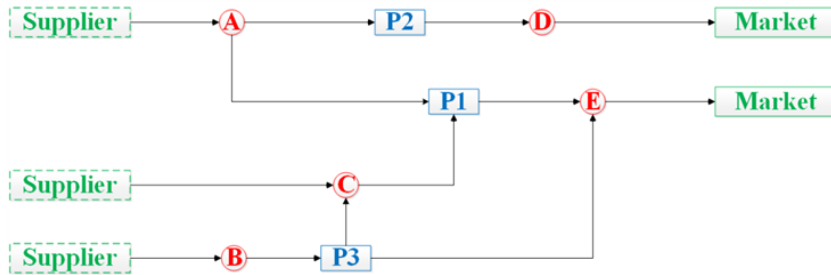


Figure 6. The chemical process network of case study 1.

The supplies of feedstocks A-C, and demands of products D-E are subject to uncertainty due to fluctuations of the market. A total of 160 demand uncertainty data are used in this case study, and each data point corresponds to a combination of all product demand realizations. For the supply uncertainty, 200 uncertainty data points are used. Each data point represents a combination

of supply uncertainty realizations for all feedstocks. There are 2 labels within demand uncertainty data, which indicates 2 data classes. There are also 2 data classes within the supply uncertainty data. The two different labels represent two kinds of government policies that encourage or discourage the industry associated with the process network in Figure 6.

By employing the proposed data-driven uncertainty modeling framework, we obtain the uncertainty modeling results for demand and supply uncertainties in Figure 7 and Figure 8, respectively. In these two figures, the red dots and red stars represent uncertainty data from different data classes, and the polytopes represent data-driven uncertainty sets with uncertainty budgets $\Phi^{\text{dem}}=1$ and $\Phi^{\text{sup}}=1$. Due to the settings of uncertainty budgets, some data points are not included in the uncertainty sets. The occurrence probabilities of different data classes are inferred from the label information, and the corresponding numerical values are listed in the two figures. From Figure 7, we can see that the probabilities of demand data classes 1 - 2 are 0.5 and 0.5, respectively. There is only one component in the Dirichlet process mixture model for both data classes 1 and 2. The proposed uncertainty model accurately captures the correlations among the two uncertain parameters for demands. Figure 8 shows that the occurrence probabilities for the two supply data classes are the same. There is one component in each of these data classes. The DDSRO problem for the planning of process network can be solved with the data-driven uncertainty information in Figure 7 and Figure 8.

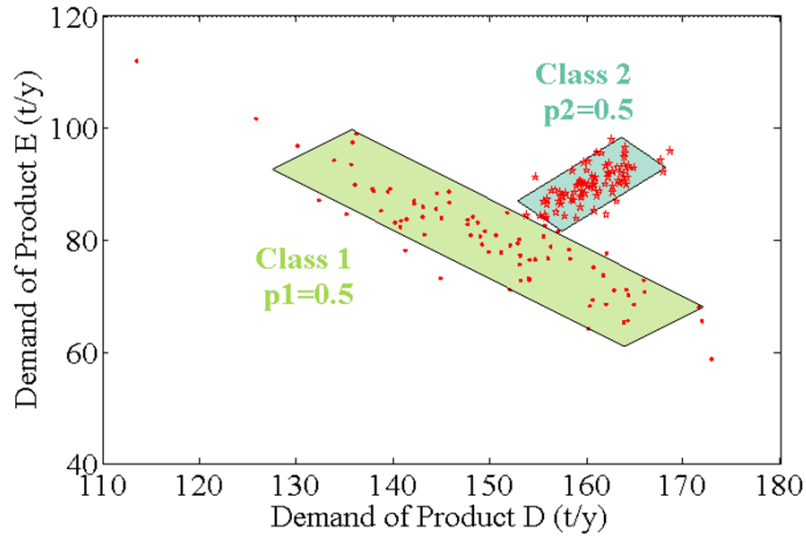


Figure 7. The data-driven demand uncertainty modeling results ($\Phi^{\text{dem}}=1$) for the two data classes in case study 1.

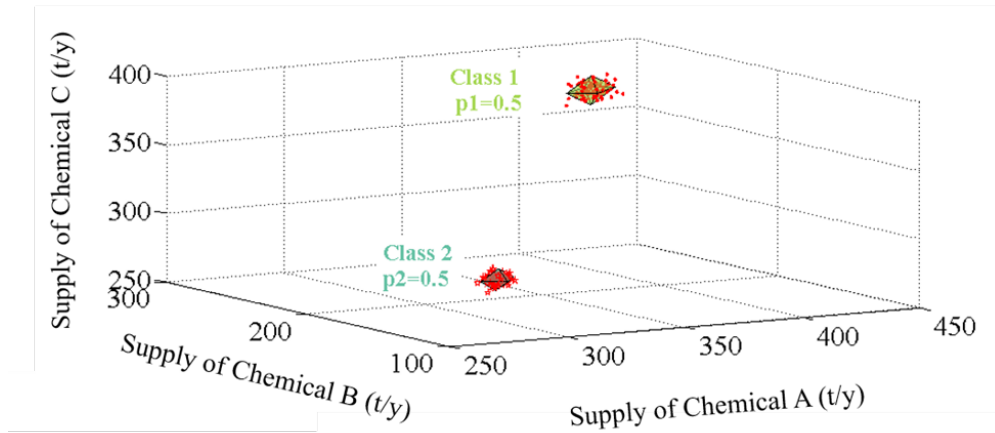


Figure 8. The data-driven supply uncertainty modeling results ($\Phi^{\text{sup}}=1$) for the two data classes in case study 1.

We solve the optimization problem of process network planning using the deterministic optimization method, the two-stage ARO method with a box set, the two-stage stochastic programming method, the DDANRO approach, and the DDSRO approach. All optimization methods are modeled in GAMS 24.7.3 [57], and are implemented on a computer with an Intel (R)

Core (TM) i7-6700 CPU @ 3.40 GHz and 32 GB RAM. The relative optimality gaps for both the tailored C&CG algorithm and the multi-cut Benders decomposition algorithm are set to be 0.1%.

The computational results and model statistics are summarized in Table 3. For the two-stage stochastic programming problem, each scenario corresponds to the combination of a demand uncertainty data point and a supply uncertainty data point. There are 32,000 (160×200) scenarios in the two-stage stochastic programming problem, and each scenario is assigned with the same probability. Two-stage stochastic programming approach aims to get a solution that performs well on average, so its objective value is only 3.7% higher than that of the DDSRO approach. However, it takes 28 iterations and 106,140 seconds to solve the resulting two-stage stochastic programming problem with the multi-cut Benders decomposition [45]. By contrast, the DDSRO problem can be solved within only 3 seconds, which demonstrates its computational advantage.

Table 3. Comparisons of model and solution statistics between different methods in in case study 1.

	Deterministic Planning	Two-stage stochastic programming		Two-stage ARO		DDANRO ($\Delta^{\text{dem}}=1, \Delta^{\text{sup}}=1$) [*]		DDSRO ($\Phi^{\text{dem}}=1, \Phi^{\text{sup}}=1$) [#]	
		Master problem	Sub-problem	Master problem	Sub-problem	Master problem	Sub-problem	Master problem	Sub-problem
Bin. Var.	30	30	0	30	5	30	20	30	20
Cont. Var.	196	32,061	131	322	386	582	1,181	582	1,181
Constraints	276	864,091	181	453	433	815	3,143	813	3,143
Max. NPV (\$K)	1,809.5		1,802.6		1,372.5		1,671.7		1,739.1
Total CPU (s)	0.2		106,140		1		7		3
Iterations	N/A		28		2		4		2

* Δ^{dem} and Δ^{sup} are data-driven uncertainty budgets in the DDANRO approach for demand and supply, respectively.

Φ^{dem} and Φ^{sup} are data-driven uncertainty budgets in the DDSRO approach for demand and supply, respectively.

The optimal capacity expansion decisions determined by the two-stage stochastic programming approach, the DDANRO method and DDSRO approach are shown in Figure 9 (a), (b) and (c), respectively. As can be observed from Figure 9, Process 1 is expanded at time period 5, and Process 2 starts the expansion at time period 2 for all the three methods. Moreover, Process 2 is further expanded at the sixth time period in the solution determined by the DDSRO approach. By contrast, Process 2 is not chosen to be expanded from time period 2 in the DDANRO solution. The optimal process capacities for the last time period determined by the two-stage stochastic programming approach, the DDANRO and DDSRO methods are listed in Table 4.

Table 4. The optimal capacity of processes at time period 10 in case study 1.

Process capacity (t/y)	Two-stage stochastic programming	DDANRO	DDSRO
Process 1	100	114	114
Process 2	227	207	225
Process 3	51	39	39

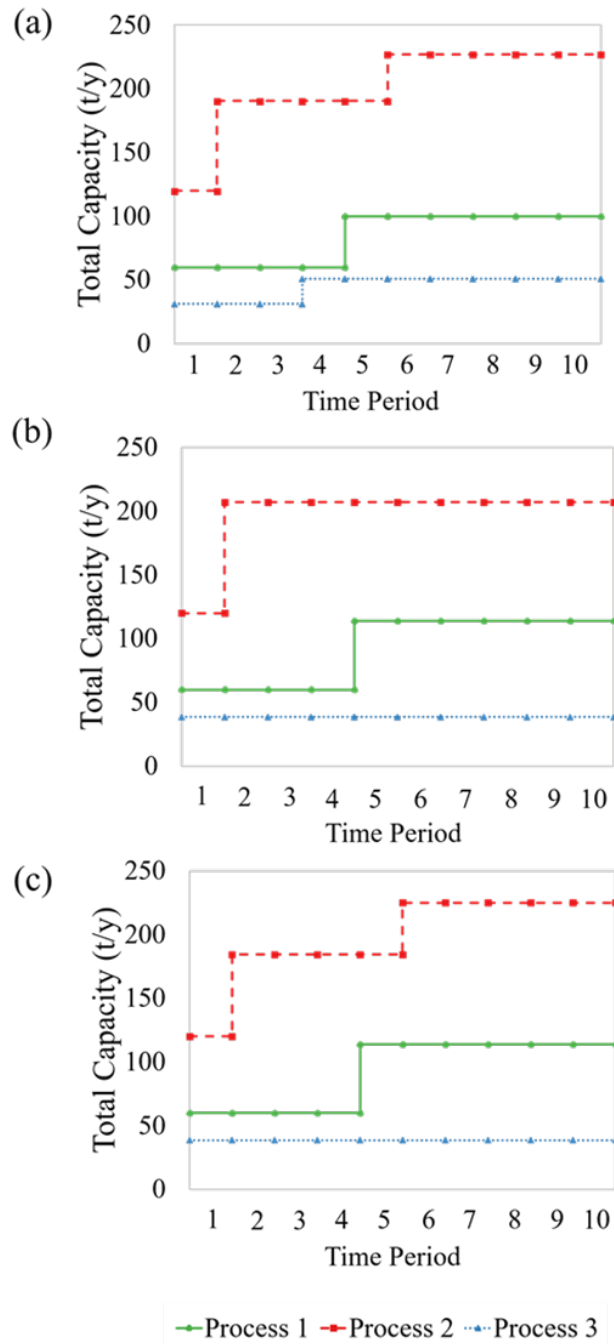


Figure 9. Optimal capacity expansion decisions over the entire planning horizon determined by (a) the two-stage stochastic programming approach, (b) the DDANRO approach, and (c) the DDSRO approach in case study 1.

Figure 10 shows revenues and cost breakdown, including fixed investment cost, variable investment cost, operating cost, and purchase cost. From the bar chart, we can see that the

deterministic method returns the highest revenue by considering only one uncertainty realization, which is the mean value of the multi-class uncertainty data. From the pie charts in Figure 10, we can observe that more than 60% of the total cost comes from feedstock purchases for all methods. Note that the percentage of the operating cost for the DDANRO method is 1% lower than those determined by the other two approaches.

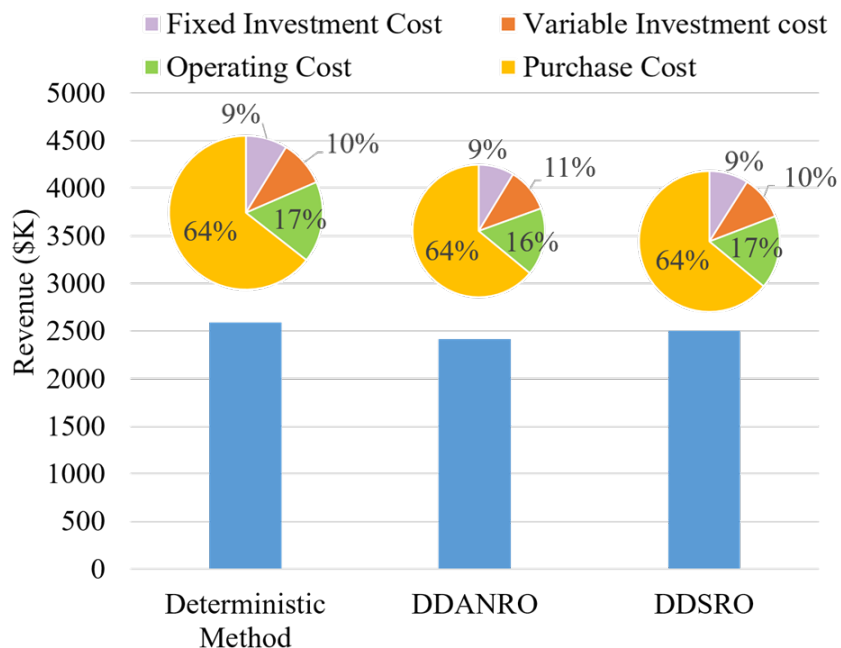


Figure 10. Revenues and cost break down determined by different methods in case study 1.

3.3. Case study 2

A large-scale case study is presented in this subsection to demonstrate the advantages of the DDSRO approach. The process network in this case study consists of 28 chemicals, 38 processes, 10 suppliers and 16 markets [53], as shown in Figure 11. In Figure 11, Chemicals A-J represent raw materials, which can be purchased from suppliers or manufactured by certain processes. Chemicals K-Z are final products, which are sold to the markets. The intermediates are denoted as AA and AB. This complex process network has such flexibility that many manufacturing options are available. For example, Chemical L can be manufactured by Process 2, Process 15 and Process 17. In this case study, we consider 10 time periods over the planning horizon, and the duration of each time period is 2 years. It is assumed that processes 12, 13, 16 and 38 have initial capacities

of 40, 25, 300 and 200 kt/y at the beginning of time period 1. These processes cannot be expanded until time period 2. The other processes can be installed at the beginning of time period 1.

As in the previous case study, supplies of all feedstocks and demands of all final products are subject to uncertainty. For the supply uncertainty, a total of 4,000 uncertainty data are used for uncertainty modeling. Each data point has 10 dimensions for a combination of all feedstocks. For the demand uncertainty, 4,000 uncertainty data points are used, and each data point is for a combination of all the 16 products. There are 3 labels within demand uncertainty data, which indicates 3 data classes. There are also 3 data classes within the supply uncertainty data. The three labels are three kinds of government policies regarding the industry associated with the process network in Figure 11: (1) encouragement policy, (2) neutral policy and (3) discouragement policy. The occurrence probabilities of different data classes are inferred from the label information. The data-driven uncertainty modeling results show that the probabilities of supply data classes 1 - 3 are 0.25, 0.50, and 0.25, respectively. There is one component in the Dirichlet process mixture models for all supply data classes. The probabilities of demand data classes 1 - 3 are calculated to be 0.25, 0.50, and 0.25, respectively. The number of components in the Dirichlet process mixture models is one for all demand data classes. The extracted uncertainty information is incorporated into the DDSRO based planning problem.

To demonstrate the advantages of the proposed approach, we solve the process network planning problem using deterministic method, the two-stage ARO approach, the two-stage stochastic programming approach, the DDANRO method and the DDSRO approach. As in the previous case study, the relative optimality gaps for the tailored C&CG algorithm and multi-cut Benders decomposition algorithm are set to be 0.1%. In the two-stage stochastic programming problem, there are $1.6E+7$ scenarios (4000×4000), and the probability of each scenario is given as $6.25E-8$. In the deterministic equivalent of the two-stage stochastic programming problem, there are 380 integer variables, 15,040,000,760 continuous variables, and 19,520,001,140 constraints. The size of this two-stage stochastic programming problem is too large to be solved within the computational time limit of 48 hours using the multi-cut Benders decomposition algorithm. Consequently, its results are not presented. The computational results and model statistics are presented in Table 5.

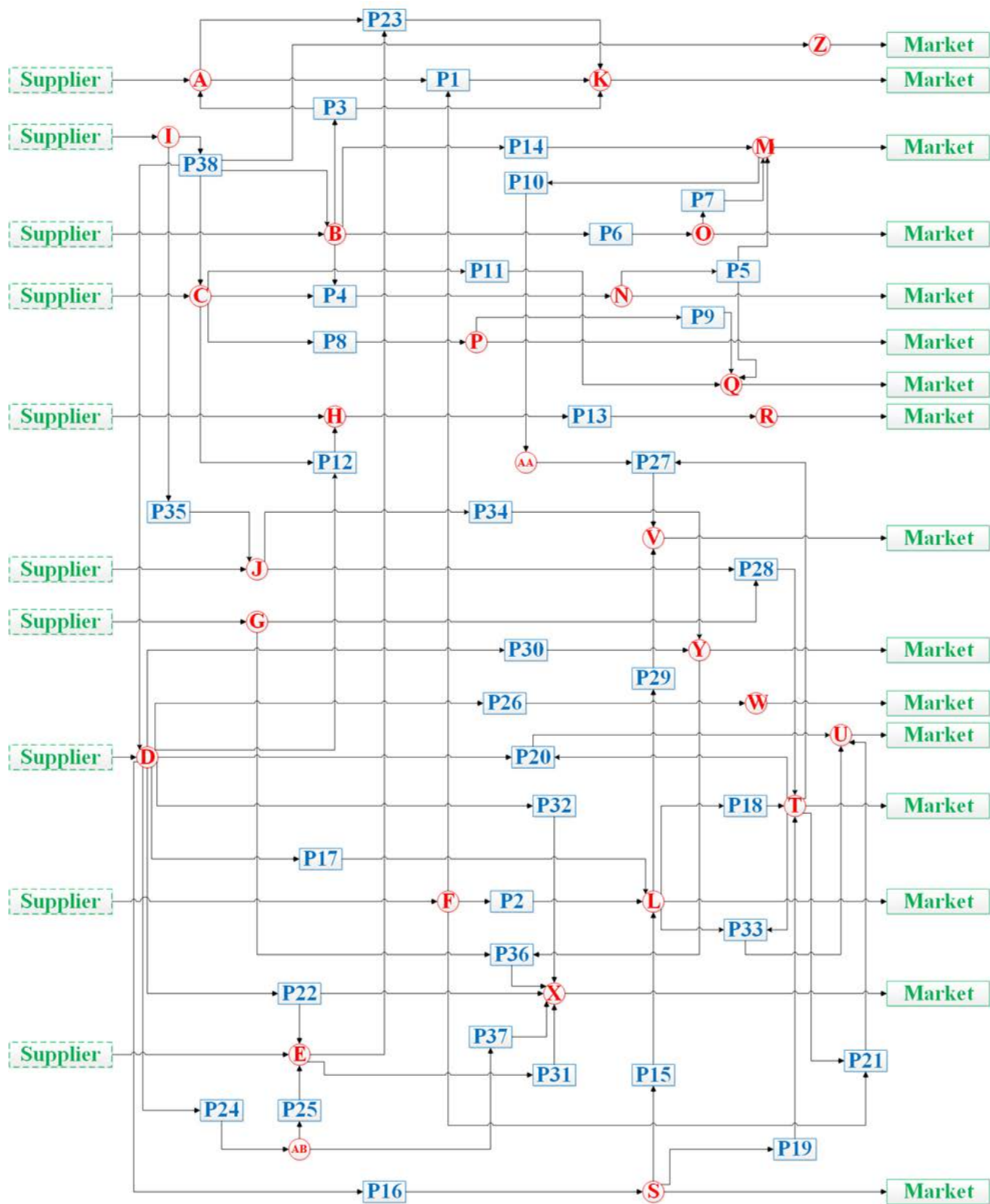


Figure 11. The chemical process network of case study 2.

Table 5. Comparisons of model and solution statistics between different methods in case study 2.

	Deterministic Planning	Two-stage ARO		DDANRO ($\Delta^{\text{dem}}=5, \Delta^{\text{sup}}=3$) [#]		DDSRO ($\Phi^{\text{dem}}=5, \Phi^{\text{sup}}=3$) [#]	
		Master problem	Sub-problem	Master problem	Sub-problem	Master problem	Sub-problem
Bin. Var.	380	380	30	380	112	380	112
Cont. Var.	1,706	6,402	2,367	13,922	32,581	120,42	32,581
Constraints	2,366	8,467	2,623	18,235	95,097	15,785	95,079
Max. NPV (\$M)	2,203.6		740.5		786.8		1,844.2
Total CPU (s)	0.4		12		3,065		557
Iterations	N/A		6		14		4

* Δ^{dem} and Δ^{sup} are data-driven uncertainty budgets in the DDANRO approach for demand and supply, respective.

Φ^{dem} and Φ^{sup} are data-driven uncertainty budgets in the DDSRO approach for demand and supply, respective.

From Table 5, we can see that the deterministic planning method consumes less computational time, and generates the highest NPV. However, its solution suffers from infeasibility issue if the supply of raw materials and demand of final products are uncertain. By leveraging the corresponding strengths of two-stage stochastic programming approach and the two-stage ARO method, the DDSRO approach generates \$1,057.4M higher NPV than the solution from the DDANRO method, while maintaining the computational tractability. The DDSRO problem can be solved within only 10 minutes using the proposed computational algorithm. The optimal design and planning decisions at period 10 determined by the deterministic optimization method, DDANRO, and DDSRO approaches are shown in Figure 12, Figure 13 and Figure 14, respectively. In these three figures, the optimal total production capacities are displayed under operating processes.

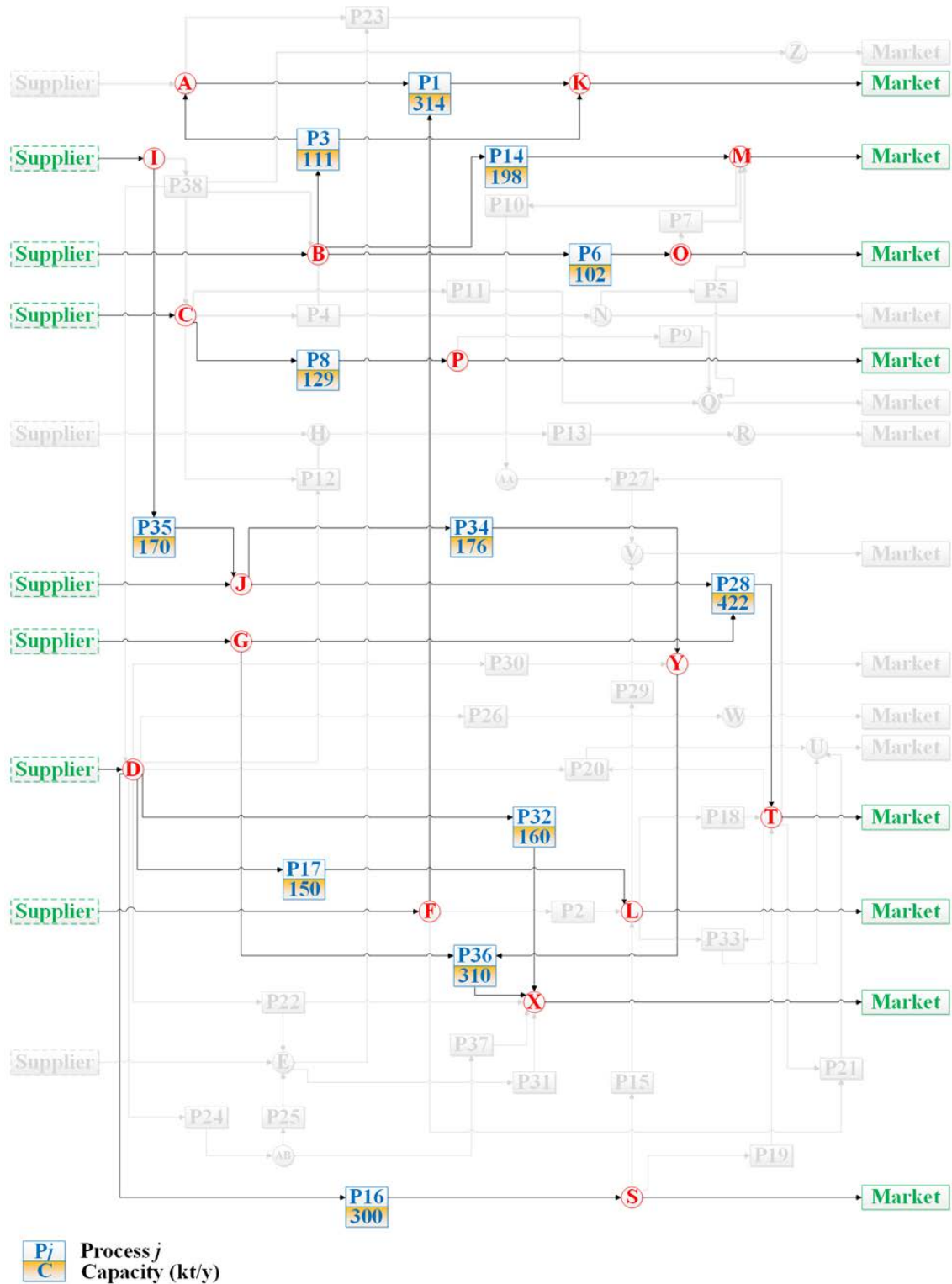


Figure 12. The optimal design and planning decisions for time period 10 determined by the deterministic optimization method in case study 2.

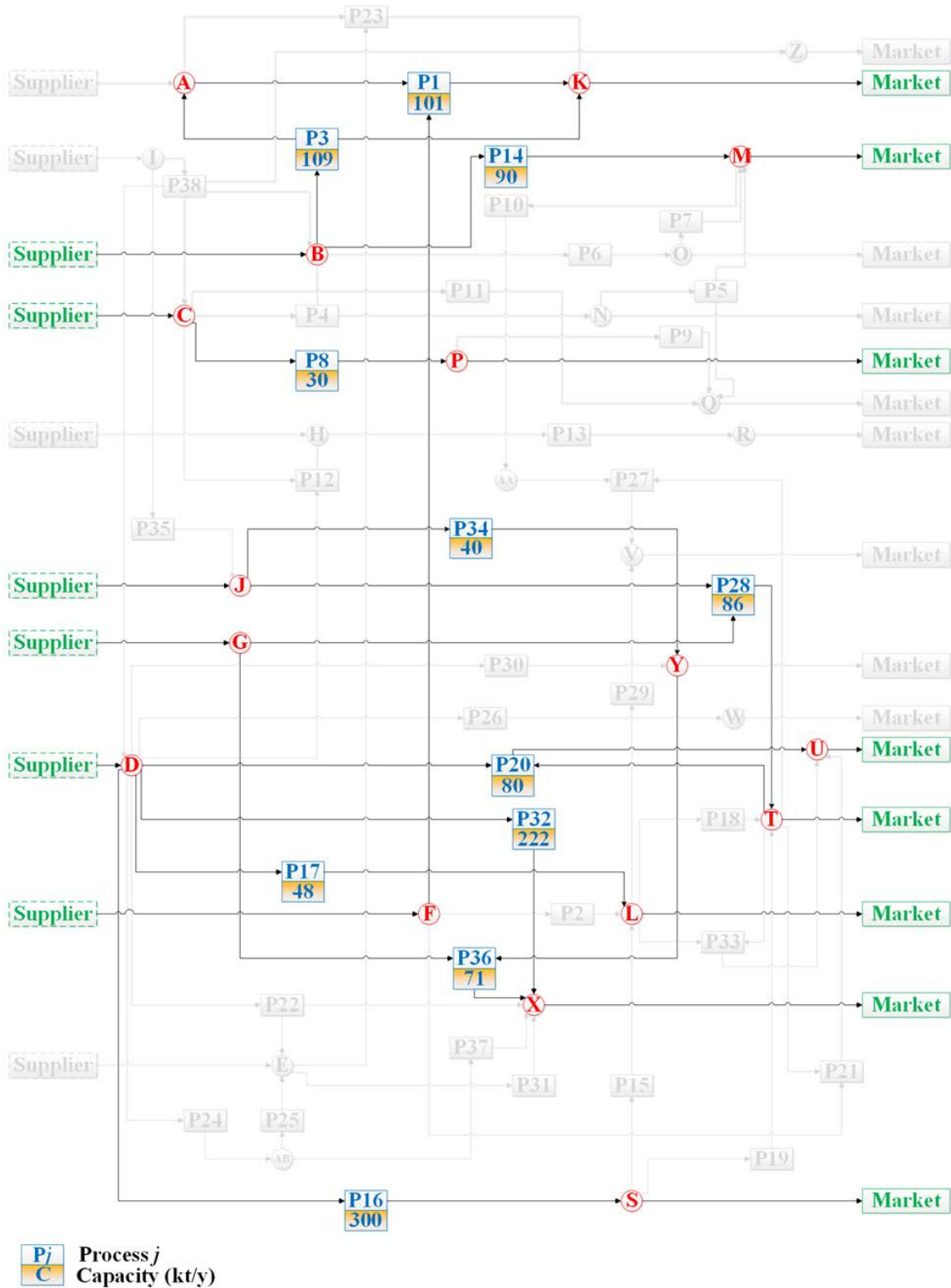


Figure 13. The optimal design and planning decisions for time period 10 determined by the DDANRO approach in case study 2.

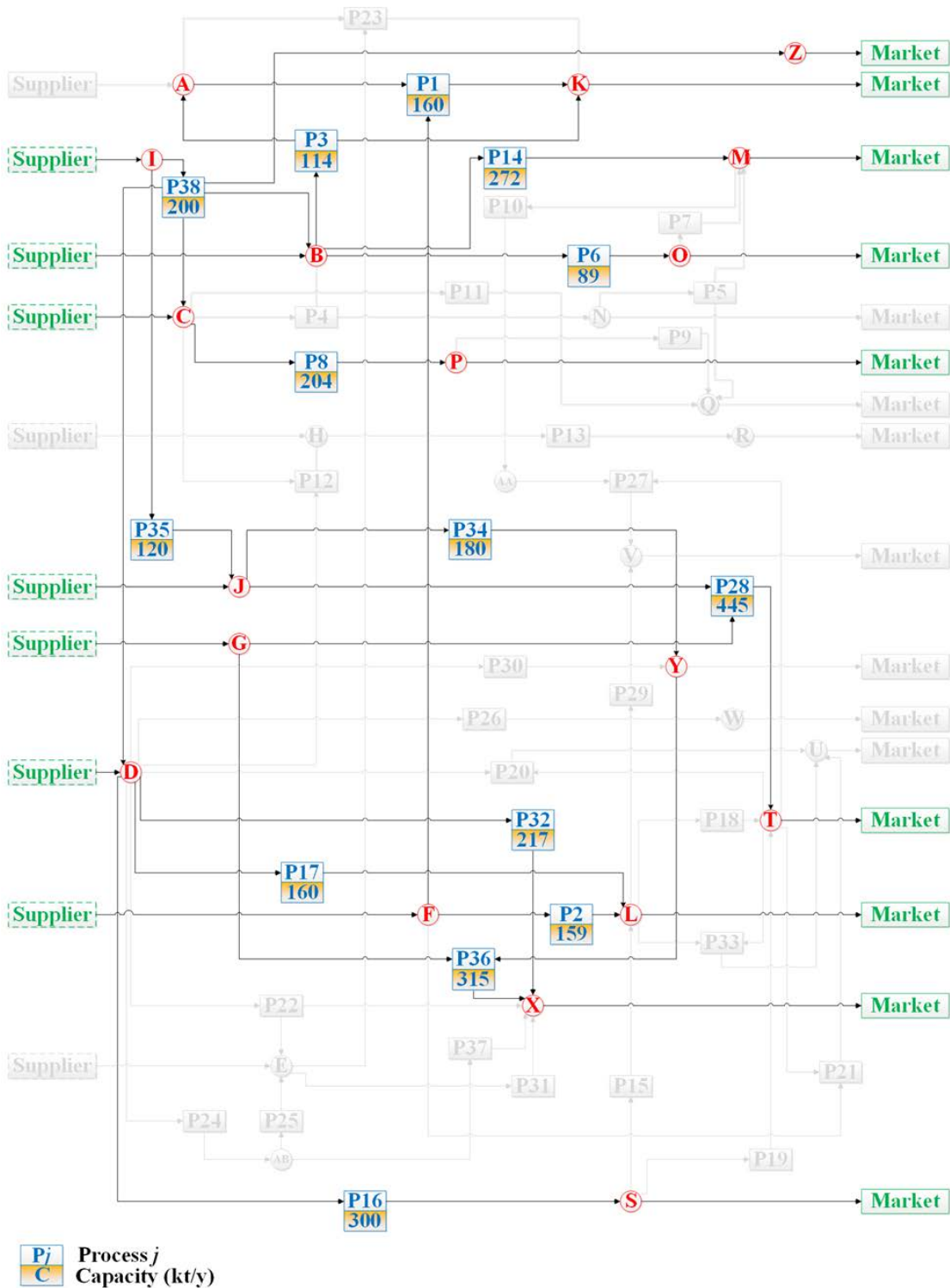


Figure 14. The optimal design and planning decisions for time period 10 determined by the proposed DDSRO approach in case study 2.

The optimal capacity expansion decisions determined by the DDANRO method and the DDSRO approach are shown in Figure 15 and Figure 16, respectively. From Figure 15, we can see that a total of 15 processes are selected in the optimal process network determined by the DDANRO method. As shown in Figure 16, a total of 18 processes are chosen in the optimal process network determined by the DDSRO approach. Specifically, Processes 2, 6 and 11 are not selected in the optimal process network determined by the DDANRO method. Besides, the optimal expansion frequencies and total capacities of Process 28 determined by the two methods are different.

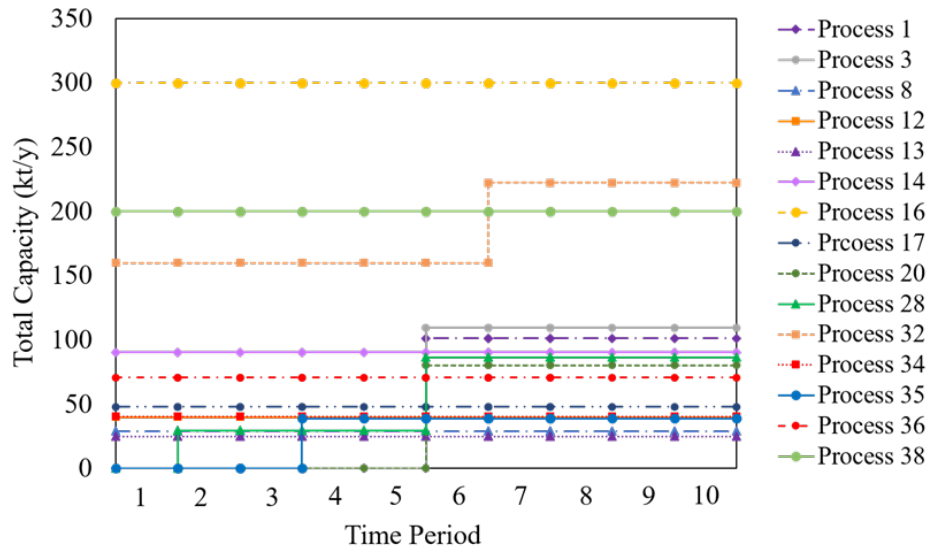


Figure 15. Optimal capacity expansion decisions over the entire planning horizon determined by the DDANRO approach in case study 2.

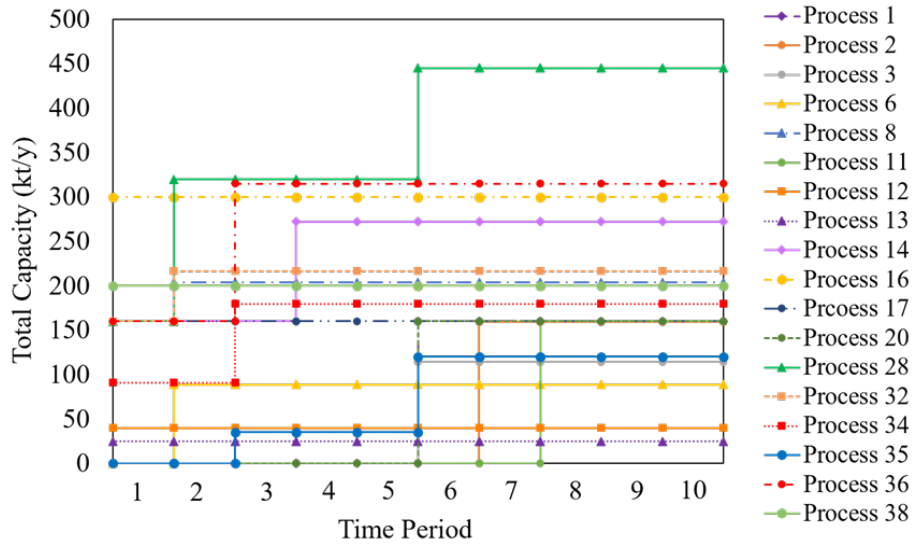


Figure 16. Optimal capacity expansion decisions over the entire planning horizon determined by the proposed DDSRO approach in case study 2.

The details on revenues and cost breakdown are shown in Figure 17. From the pie charts in Figure 17, we can see that more than half of the total cost is from purchasing raw materials for the three approaches. The investment costs for the deterministic method, the DDANRO and DDSRO methods are \$338.4M, \$142.3M and \$323.1M, respectively. The lower capital costs of the DDANRO method can be explained by the fewer selected processes and the lower capacities compared with the other two methods.

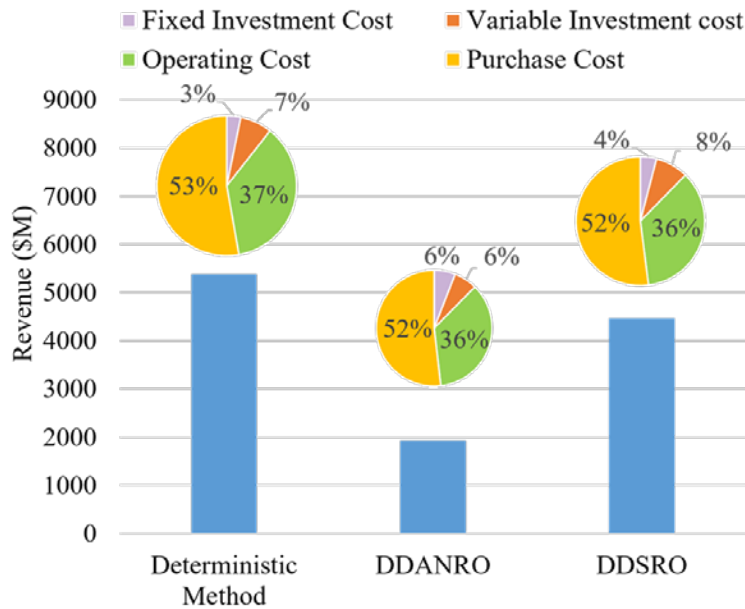


Figure 17. Revenues and cost break down determined by different methods in case study 2.

To demonstrate the superior performance of the DDSRO approach over the DDANRO method in an uncertain environment, we perform a simulation with randomly generated 1,000 uncertainty realizations. These 1,000 uncertainty realizations are generated in exactly the same way as we generate the original uncertainty data points for uncertainty modeling. Specifically, the “testing” uncertainty realizations are from the same 3 data classes as the uncertainty data used for data-driven uncertainty modeling, and the probability distribution for each data class is also the same to ensure that the uncertainty data for modeling and for simulation are independently and identically distributed. The simulation results are shown in Figure 18, in which the X-axis denotes the index of uncertainty realizations, and the Y-axis denotes the NPV. The statistics of the simulation results are provided in Table 6. In the figure, the green stars represent the DDANRO solutions, while the brown rhombuses represent the DDSRO solutions. The DDSRO approach generates a higher NPV than that of the DDANRO method under 786 out of 1,000 uncertainty realizations. We also plot the average NPV over all the 1,000 uncertainty realizations for the DDANRO and DDSRO approaches, as given by the red dashed horizontal line and blue horizontal line, respectively. The DDSRO approach generates \$931.4M higher expected NPV than that of the DDANRO method, while the worst-case NPV is merely \$78.4M lower compared with that of the DDANRO method. The above simulation results clearly demonstrate that the DDSRO approach compares favorably with the DDANRO method in handling labeled multi-class uncertainty data.

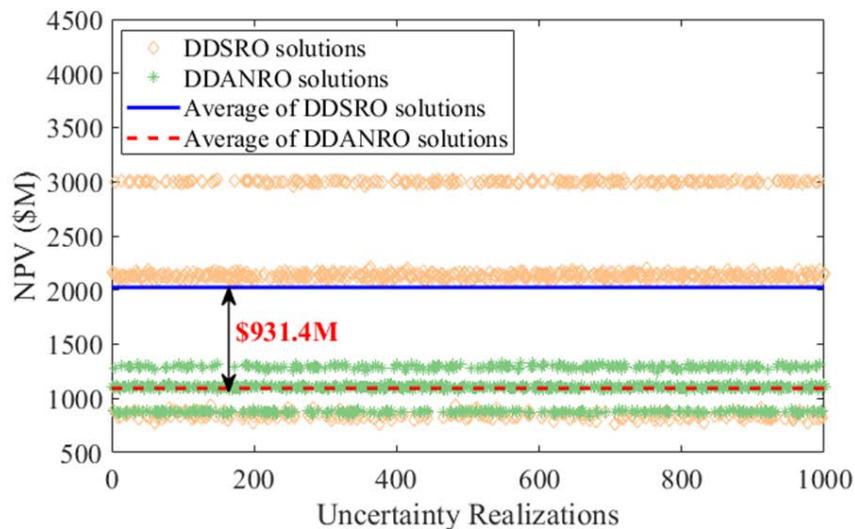


Figure 18. Simulation results for the DDANRO and DDSRO approaches with randomly generated 1,000 “testing” uncertainty realizations that are independently and identically distributed as the uncertainty data used for data-driven uncertainty modeling in case study 2.

Table 6. Summary of the simulation results in case study 2.

	Two-stage ARO	DDANRO	DDSRO
Expected NPV (\$M)	959.7	1,093.2	2,024.6
Worst-case NPV (\$M)	745.3	839.6	761.2
Standard deviation of NPV (\$M)	123.7	145.8	761.1

Figure 19 displays the upper and lower bounds in each iteration of the proposed algorithm. The X-axis and Y-axis denote the iteration number and the objective function values, respectively. In Figure 19, the green dots stand for the upper bounds, while the yellow circles represent the lower bounds. The proposed solution algorithm requires only 4 iterations to converge. During the first two iterations, the relative optimality gap decreases significantly from 88.01% to 0.67%. The results demonstrate the efficiency of the proposed computational algorithm.

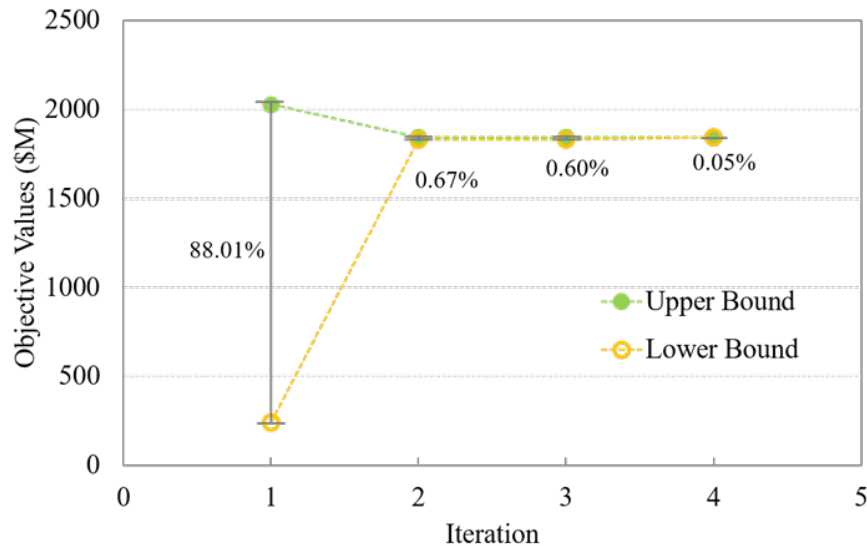


Figure 19. Upper and lower bounds in each iteration of the tailored C&CG algorithm in case study 2.

To investigate how the optimal solution varies with the uncertainty budget parameters, a heat map of solutions under different supply and demand budgets is shown in Figure 20. It is clear to see that increasing either the supply or demand uncertainty budget decreases the NPV. We can see that increasing the uncertainty budget for supply does not change the objective value significantly. Moreover, increasing the uncertainty budget for demands reduces the NPV considerably.

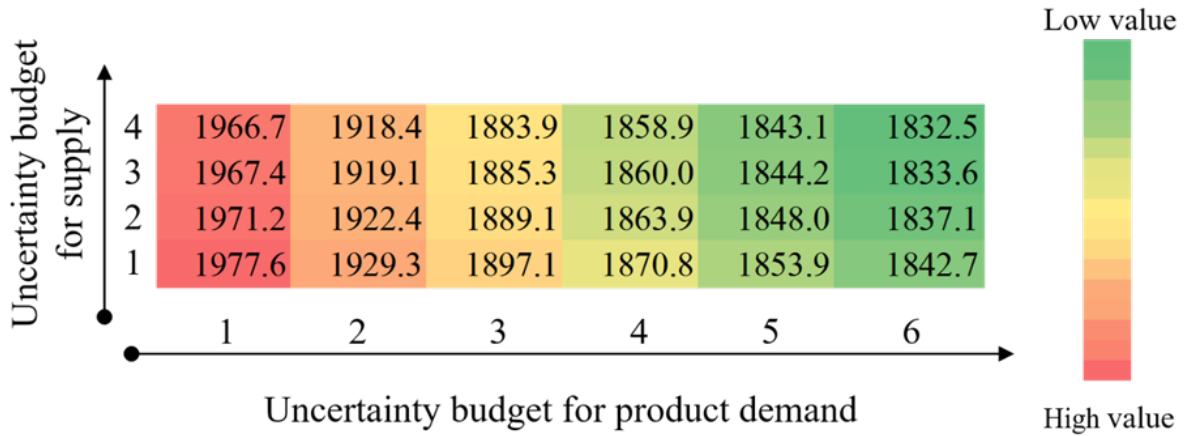


Figure 20. Heat map of solutions under different budgets for the DDSRO approach in case study 2.

4. Conclusions

In this paper, a novel DDSRO framework was proposed for labeled multi-class uncertainty data. Instead of handling all uncertainty data homogeneously, the proposed framework explicitly accounted for the label information in the proposed multi-level optimization model. The probability distribution for data classes was learned from uncertainty data through maximum likelihood estimation. A group of Dirichlet process mixture models were used to construct uncertainty sets for each data class. The proposed data-driven uncertainty model was capable of automatically adapting its complexity based on data structure, thus accurately extracting the useful information from uncertainty data. Two-stage stochastic programming approach was nested in the outer optimization problem, aiming to balance different data classes based on their occurrence probabilities. To handle uncertainties in each data class, robust optimization was nested in the inner optimization problem for the robustness of the solution and computational tractability. The proposed DDSRO framework leveraged the advantages of two-stage stochastic programming approach and robust optimization, and at the same time exploited the value of big data. Since the resulting DDSRO problem has multi-level structure, we further proposed a tailored C&CG algorithm to address the computational challenge. We presented two case studies on strategic planning of process networks under supply and demand uncertainties. The results showed that the DDSRO approach was advantageous over the DDANRO method in handling labeled multi-class uncertainty data.

Acknowledgments

The authors acknowledge financial support from the National Science Foundation (NSF) CAREER Award (CBET-1643244).

Appendix A: Dirichlet Process Mixture Model

The Dirichlet process is a widely used stochastic process, especially in the Dirichlet process mixture model. Suppose a random distribution G follows a Dirichlet process, denoted as $G \sim DP(\alpha, G_0)$, $(G(\Theta_1), \dots, G(\Theta_r))$ is then Dirichlet distributed for any measurable partition $(\Theta_1, \dots, \Theta_r)$ of Θ [58].

$$(G(\Theta_1), \dots, G(\Theta_r)) \sim Dir(\alpha G_0(\Theta_1), \dots, \alpha G_0(\Theta_r)) \quad (A1)$$

where α and G_0 are the concentration parameter and base distribution, respectively. *Dir* in (A1) represents the Dirichlet distribution. A random draw from the Dirichlet process follows the stick-breaking construction in (A2) [59].

$$G = \sum_{k=1}^{\infty} \pi_k \delta_{\theta_k} \quad (A2)$$

where $\pi_k = \beta_k \prod_{j=1}^{k-1} (1 - \beta_j)$, β_k is the proportion of stick broken off from the remaining stick, and $\beta_k \sim Beta(1, \alpha)$. θ_k is the random variable drawn from the base distribution G_0 . The delta function δ_{θ_k} is equal to 1 at the location of θ_k , and becomes 0 elsewhere.

In the Dirichlet process mixture model, θ_k is treated as the parameters of the data distribution. A significant feature of the Dirichlet process mixture model is that it has a potentially infinite number of components. This novel feature grants it with great flexibility to model intricate data distribution. The Dirichlet process mixture model is given in (A3) [49].

$$\begin{aligned} \beta_k &| \alpha \sim Beta(1, \alpha) \\ \theta_k &| G_0 \sim G_0 \\ t_i &| \{\beta_1, \beta_2, \dots\} \sim Mult(\pi(\beta)) \\ o_i &| t_i \sim p(o_i | \theta_{t_i}) \end{aligned} \quad (A3)$$

where *Beta* and *Mult* denote Beta distribution and multinomial distribution, respectively. The observation is denoted as o_i drawn from the t_i th component.

Appendix B: Details of The Proposed Computational Algorithm

The multi-level optimization problem (17) can be reformulated to an equivalent single-level optimization problem by enumerating all the extreme points [60]. However, this single-level optimization problem could be a large-scale optimization problem due to the potentially large number of extreme points. Therefore, we partially enumerate the extreme points, and construct the master problem. Because master problem **(MP)** contains a subset of the extreme points, it is a relaxation of the original single-level optimization problem. The master problem **(MP)** is shown below.

$$\begin{aligned}
 & \min_{\mathbf{x}, \eta, \mathbf{y}_s^l} \mathbf{c}^T \mathbf{x} + \eta \\
 & \text{s.t. } \mathbf{Ax} \geq \mathbf{d} \\
 \text{(MP)} \quad & \eta \geq \sum_s p_s \left(\mathbf{b}^T \mathbf{y}_s^l \right), \quad l=1, \dots, r \\
 & \mathbf{Tx} + \mathbf{Wy}_s^l \geq \mathbf{h} - \mathbf{Mu}_s^l, \quad l=1, \dots, r, \forall s \\
 & \mathbf{x} \in \mathbb{R}_+^{n_1} \times \mathbb{Z}^{n_2}, \quad \mathbf{y}_s^l \in \mathbb{R}_+^{n_3}, \quad l=1, \dots, r, \forall s
 \end{aligned}$$

where s is the index for data class, and \mathbf{u}_s^l is the enumerated uncertainty realization at the l th iteration for data class s , \mathbf{y}_s^l is its corresponding recourse variable, and r stands for the current number of iterations.

To enumerate the important uncertainty realization on-the-fly, the sub-problem in (B1) is solved in each iteration.

$$\begin{aligned}
 Q_{s,i}(\mathbf{x}) &= \max_{\mathbf{u} \in U_{s,i}} \min_{\mathbf{y}_s} \mathbf{b}^T \mathbf{y}_s \\
 & \text{s.t. } \mathbf{Wy}_s \geq \mathbf{h} - \mathbf{Tx} - \mathbf{Mu} \\
 & \mathbf{y}_s \in \mathbb{R}_+^{n_3}
 \end{aligned} \tag{B1}$$

It is worth noting that (B1) is a max-min optimization problem, which can be transformed to a single-level optimization problem by employing strong duality or KKT conditions. To make the sub-problem computationally tractable, we dualize the inner optimization problem of (B1), which is a linear program with regard to \mathbf{y}_s , and merge the dual problem with the maximization problem with respect to \mathbf{u} . The resulting problem is shown below.

$$\begin{aligned}
Q_{s,i}(\mathbf{x}) &= \max_{\mathbf{z}, \boldsymbol{\varphi}} (\mathbf{h} - \mathbf{T}\mathbf{x} - \mathbf{M}\boldsymbol{\mu}_{s,i})^T \boldsymbol{\varphi} - \sum_t \sum_j (\kappa_{s,i} \mathbf{M} \boldsymbol{\Psi}_{s,i}^{1/2} \Lambda_{s,i})_{tj} \mathbf{z}_j \boldsymbol{\varphi}_t \\
(\text{SUP}_{s,i}) \quad & \text{s.t. } \mathbf{W}^T \boldsymbol{\varphi} \leq \mathbf{b} \\
& \boldsymbol{\varphi} \geq \mathbf{0} \\
& \|\mathbf{z}\|_\infty \leq 1, \|\mathbf{z}\|_1 \leq \Phi_{s,i}
\end{aligned}$$

where $\boldsymbol{\varphi}$ is the vector of dual variables corresponding to the constraint $\mathbf{W}\mathbf{y} \geq \mathbf{h} - \mathbf{T}\mathbf{x} - \mathbf{M}\mathbf{u}$, $\boldsymbol{\varphi}_t$ represents the t th component in vector $\boldsymbol{\varphi}$, and \mathbf{z}_j is the j th component in vector \mathbf{z} . Problem (SUP_{s,i}) is reformulated to handle the bilinear term $\mathbf{z}_j \boldsymbol{\varphi}_t$ in its objective function. After solving the subproblem, a new extreme point is identified to be added to the master problem along with its corresponding second-stage decision.

To facilitate the reformulation, \mathbf{z}_j is divided into two parts $\mathbf{z}_j = \mathbf{z}_j^+ - \mathbf{z}_j^-$. Thus, we have

$$\mathbf{u} = \boldsymbol{\mu}_{s,i} + \kappa_{s,i} \boldsymbol{\Psi}_{s,i}^{1/2} \Lambda_{s,i} (\mathbf{z}^+ - \mathbf{z}^-) \quad (\text{B2})$$

Following the existing literature [61, 62], the uncertainty budget parameter $\Phi_{s,i}$ is typically set as an integer value due to its physical meaning. For the integer uncertainty budget, the optimal \mathbf{z}_j^+ and \mathbf{z}_j^- take the values of 0 or 1, and these two variables can be restricted to binary variables. We employ Glover's linearization for the bilinear terms $\mathbf{G}_{ij}^+ = \mathbf{z}_j^+ \boldsymbol{\varphi}_t$ and $\mathbf{G}_{ij}^- = \mathbf{z}_j^- \boldsymbol{\varphi}_t$ [63], which are the products of a binary variable \mathbf{z}_j^+ (and \mathbf{z}_j^-) and a continuous variable $\boldsymbol{\varphi}_t$, and reformulate (SUP_{s,i}) into (B3).

$$\begin{aligned}
Q_{s,i}(\mathbf{x}) &= \max_{\boldsymbol{\varphi}, \mathbf{z}^+, \mathbf{z}^-, \mathbf{G}^+, \mathbf{G}^-} (\mathbf{h} - \mathbf{T}\mathbf{x} - \mathbf{M}\boldsymbol{\mu}_{s,i})^T \boldsymbol{\varphi} - \text{Tr} \left((\kappa_{s,i} \mathbf{M} \boldsymbol{\Psi}_{s,i}^{1/2} \Lambda_{s,i})^T (\mathbf{G}^+ - \mathbf{G}^-) \right) \\
\text{s.t. } & \mathbf{W}^T \boldsymbol{\varphi} \leq \mathbf{b} \\
& \boldsymbol{\varphi} \geq \mathbf{0} \\
& \mathbf{0} \leq \mathbf{G}^+ \leq \boldsymbol{\varphi} \cdot \mathbf{e}^T \\
& \mathbf{0} \leq \mathbf{G}^- \leq \boldsymbol{\varphi} \cdot \mathbf{e}^T \\
& \mathbf{G}^+ \leq \tilde{\mathbf{e}} \cdot (M_0 \cdot \mathbf{z}^+)^T \\
& \mathbf{G}^- \leq \tilde{\mathbf{e}} \cdot (M_0 \cdot \mathbf{z}^-)^T \\
& \mathbf{G}^+ \geq \boldsymbol{\varphi} \cdot \mathbf{e}^T - \tilde{\mathbf{e}} \cdot (M_0 \cdot (\mathbf{e} - \mathbf{z}^+))^T \\
& \mathbf{G}^- \geq \boldsymbol{\varphi} \cdot \mathbf{e}^T - \tilde{\mathbf{e}} \cdot (M_0 \cdot (\mathbf{e} - \mathbf{z}^-))^T \\
& \mathbf{e}^T (\mathbf{z}^+ + \mathbf{z}^-) \leq \Phi_{s,i} \\
& \mathbf{z}^+ + \mathbf{z}^- \leq \mathbf{e}, \quad \mathbf{z}^+, \mathbf{z}^- \in \{0, 1\}^K
\end{aligned} \quad (\text{B3})$$

where \mathbf{e} and $\tilde{\mathbf{e}}$ denote vectors with all elements being one. The dimensions of these two vectors are $\dim(\mathbf{e}) = \dim(\mathbf{u}) = K$ and $\dim(\tilde{\mathbf{e}}) = \dim(\boldsymbol{\phi})$. The t th row and j th column elements of matrices \mathbf{G}^+ and \mathbf{G}^- are \mathbf{G}_{ij}^+ and \mathbf{G}_{ij}^- , respectively. The notation Tr represents the trace of a matrix.

Appendix C: Supplementary Data for Case Study 1

Table C1. Mass balance relationships for processes in case study 1.

Process	Mass balance relationship
Process 1	0.63 A + 0.58 C → E
Process 2	0.64 A → D
Process 3	1.25 B → 0.9 C + E

Table C2. Fixed investment costs (10^2 \$) for processes in case study 1.

Process	Period 1	Period 2	Period 3	Period 4	Period 5	Period 6	Period 7	Period 8	Period 9	Period 10
Process 1	337.0	260.0	200.0	150.0	120.0	80.0	70.0	90.0	120.0	150.0
Process 2	125.0	120.0	101.0	121.0	121.0	125.0	120.0	101.0	141.0	181.0
Process 3	61.0	61.0	30.0	20.0	15.0	50.0	51.0	40.0	20.0	60.0

Table C3. Variable investment costs (10^2 \$/t) for processes in case study 1.

Process	Period 1	Period 2	Period 3	Period 4	Period 5	Period 6	Period 7	Period 8	Period 9	Period 10
Process 1	3.7	3.6	4.0	2.0	1.0	2.2	2.6	2.5	2.4	3.0
Process 2	2.5	2.4	2.9	5.2	3.0	1.5	2.4	2.9	2.2	4.0
Process 3	3.1	3.0	3.3	2.4	2.0	1.1	3.0	3.3	2.4	2.0

Table C4. Purchase prices (10^2 \$/t) for chemicals in case study 1.

Chemicals	Period 1	Period 2	Period 3	Period 4	Period 5	Period 6	Period 7	Period 8	Period 9	Period 10
A	8.2	9.0	5.5	5.0	5.2	4.2	3.0	4.5	3.0	5.0
B	4.0	3.3	3.2	2.0	2.0	2.0	3.3	2.2	3.0	2.0
C	1.5	1.3	1.2	1.1	1.2	1.5	1.3	1.2	1.1	1.2
D	0.0	0.0	0.0	0.0	0.0	0.0	0.0	0.0	0.0	0.0
E	0.0	0.0	0.0	0.0	0.0	0.0	0.0	0.0	0.0	0.0

Table C5. Sale prices (10^2 \$/t) for chemicals in case study 1.

Chemicals	Period 1	Period 2	Period 3	Period 4	Period 5	Period 6	Period 7	Period 8	Period 9	Period 10
A	0.0	0.0	0.0	0.0	0.0	0.0	0.0	0.0	0.0	0.0
B	0.0	0.0	0.0	0.0	0.0	0.0	0.0	0.0	0.0	0.0
C	0.0	0.0	0.0	0.0	0.0	0.0	0.0	0.0	0.0	0.0
D	15.4	14.0	16.5	17.3	18.5	22.4	32.0	34.5	21.3	22.5
E	12.8	12.0	15.0	18.0	25.0	28.8	23.0	21.0	22.0	22.0

Table C6. Operating costs (10^2 \$/t) for processes in case study 1.

Process	Period 1	Period 2	Period 3	Period 4	Period 5	Period 6	Period 7	Period 8	Period 9	Period 10
Process 1	0.8	0.5	0.4	0.6	0.4	0.3	0.3	0.4	0.3	0.3
Process 2	1.5	1.6	1.5	1.0	1.0	0.8	0.6	0.5	1.0	1.0
Process 3	1.5	1.2	1.0	0.8	0.8	0.9	1.5	1.2	0.8	1.5

Appendix D: Supplementary Data for Case Study 2

Table D1. Mass balance relationships for processes in case study 2.

Process	Mass balance relationship	Process	Mass balance relationship
Process 1	$0.58 A + 0.63 F \rightarrow K$	Process 20	$0.35 D + 0.71 T \rightarrow U$
Process 2	$0.64 F \rightarrow L$	Process 21	$0.32 F + 0.72 T \rightarrow U$
Process 3	$1.25 B \rightarrow 0.055 A + K$	Process 22	$0.88 D \rightarrow E + 0.03 X$
Process 4	$0.4 B + 0.69 C \rightarrow N$	Process 23	$0.56 A + 0.92 E \rightarrow K$
Process 5	$2.3 N \rightarrow M + 1.7 Q$	Process 24	$0.39 D \rightarrow AB$
Process 6	$0.74 B \rightarrow O$	Process 25	$1.97 AB \rightarrow E$
Process 7	$1.1 O \rightarrow M$	Process 26	$0.3 D \rightarrow W$
Process 8	$C \rightarrow P$	Process 27	$0.65 T + 0.46 AB \rightarrow V$
Process 9	$1.26 P \rightarrow Q$	Process 28	$0.56 G + 0.56 J \rightarrow T$
Process 10	$1.57 M \rightarrow AA$	Process 29	$1.2 L \rightarrow V$
Process 11	$1.01 C \rightarrow Q$	Process 30	$1.17 D \rightarrow Y$
Process 12	$0.76 C + 0.28 D \rightarrow H$	Process 31	$0.75 E \rightarrow X$
Process 13	$1.14 H \rightarrow R$	Process 32	$0.53 D \rightarrow X$
Process 14	$0.78 B \rightarrow M$	Process 33	$0.6 L + 0.82 T \rightarrow U$
Process 15	$1.34 S \rightarrow L$	Process 34	$0.42 J \rightarrow Y$
Process 16	$0.6 D \rightarrow S$	Process 35	$0.5 I \rightarrow J$
Process 17	$0.67 D \rightarrow L$	Process 36	$0.53 G + 0.57 Y \rightarrow X$
Process 18	$1.1 L \rightarrow T$	Process 37	$1.44 AB \rightarrow X$
Process 19	$0.98 S \rightarrow T$	Process 38	$3.08 I \rightarrow 0.38 B + 0.22 C + D$

Table D2. Fixed investment costs (10^5 \$) for processes in case study 2.

Process	Period 1	Period 2	Period 3	Period 4	Period 5	Period 6	Period 7	Period 8	Period 9	Period 10
Process 1	337.1	260.0	200.0	150.0	120.0	50.0	60.0	30.0	150.0	150.0
Process 2	125.0	120.0	101.0	121.0	121.0	125.0	20.0	101.0	41.0	81.0
Process 3	321.0	311.0	300.0	200.0	250.0	121.0	111.0	100.0	100.0	150.0
Process 4	80.8	71.0	66.0	77.0	77.0	80.8	21.0	66.0	77.0	77.0
Process 5	96.6	90.0	85.0	84.0	84.0	96.6	20.0	85.0	84.0	84.0
Process 6	162.0	60.0	55.0	43.0	43.0	162.0	60.0	15.0	43.0	43.0
Process 7	105.0	98.0	67.0	56.0	56.0	105.0	98.0	17.0	56.0	56.0
Process 8	102.0	82.0	73.0	60.0	80.0	102.0	82.0	83.0	110.0	110.0
Process 9	115.0	105.0	145.0	140.0	140.0	15.0	15.0	145.0	140.0	140.0
Process 10	17.5	16.0	23.0	21.0	21.0	17.5	16.0	23.0	21.0	21.0
Process 11	118.0	107.0	118.0	109.0	109.0	18.0	107.0	18.0	19.0	19.0
Process 12	50.0	40.0	50.0	150.0	50.0	50.0	40.0	50.0	150.0	50.0
Process 13	237.0	227.0	238.0	241.0	241.0	137.0	127.0	138.0	141.0	141.0
Process 14	52.9	54.0	40.0	30.0	30.0	52.9	54.0	40.0	30.0	30.0
Process 15	120.0	113.0	114.0	101.0	114.0	120.0	113.0	114.0	101.0	114.0
Process 16	37.0	40.0	51.0	60.0	60.0	37.0	40.0	51.0	60.0	60.0
Process 17	110.0	120.0	101.0	98.0	101.0	110.0	120.0	101.0	98.0	101.0
Process 18	40.0	50.0	48.0	32.0	32.0	40.0	50.0	48.0	32.0	32.0
Process 19	42.0	43.0	40.0	20.0	40.0	42.0	43.0	40.0	20.0	40.0
Process 20	75.0	60.0	54.0	50.0	50.0	75.0	60.0	54.0	50.0	50.0
Process 21	75.0	60.0	50.0	60.0	60.0	75.0	60.0	50.0	60.0	60.0
Process 22	101.0	100.0	92.0	81.0	81.0	101.0	100.0	92.0	81.0	81.0
Process 23	353.0	342.0	350.0	291.0	291.0	353.0	342.0	350.0	291.0	291.0
Process 24	150.0	140.0	120.0	141.0	141.0	150.0	140.0	120.0	141.0	141.0
Process 25	130.0	120.0	143.0	122.0	122.0	130.0	120.0	143.0	122.0	122.0
Process 26	85.0	75.0	68.0	71.0	71.0	85.0	75.0	68.0	71.0	71.0
Process 27	25.0	14.0	21.0	19.0	21.0	25.0	14.0	21.0	19.0	21.0
Process 28	61.0	32.0	34.0	29.0	19.0	11.0	12.0	10.0	9.0	10.0
Process 29	27.0	16.0	16.0	18.0	18.0	27.0	16.0	16.0	18.0	18.0
Process 30	120.0	118.0	116.0	119.0	119.0	120.0	118.0	116.0	119.0	119.0
Process 31	87.0	90.0	81.0	80.0	80.0	87.0	90.0	81.0	80.0	80.0
Process 32	85.0	91.0	89.0	80.0	80.0	85.0	91.0	89.0	80.0	80.0
Process 33	80.0	70.0	61.0	52.0	52.0	80.0	70.0	61.0	52.0	52.0
Process 34	111.0	100.0	80.0	80.0	80.0	111.0	100.0	80.0	80.0	80.0
Process 35	54.0	60.0	45.0	43.0	43.0	54.0	60.0	45.0	43.0	43.0
Process 36	89.0	91.0	90.0	100.0	100.0	89.0	91.0	90.0	100.0	40.0
Process 37	131.0	120.0	100.0	151.0	100.0	31.0	20.0	100.0	51.0	40.0
Process 38	12.8	9.0	8.0	4.0	9.0	12.8	9.0	8.0	4.0	9.0

Table D3. Variable investment costs (10^2 \$/t) for processes in case study 2.

Process	Period 1	Period 2	Period 3	Period 4	Period 5	Period 6	Period 7	Period 8	Period 9	Period 10
Process 1	3.7	3.6	4.0	2.0	1.0	0.2	0.6	0.5	0.4	3.0
Process 2	2.5	2.4	2.9	5.2	3.0	1.5	0.4	2.9	0.2	4.0
Process 3	3.1	3.0	3.3	0.4	2.0	0.1	3.0	3.3	4.4	2.0
Process 4	1.0	0.5	0.5	0.6	0.5	0.2	0.5	0.1	0.1	0.1
Process 5	2.1	2.0	2.0	0.1	1.0	1.1	2.0	1.0	2.1	1.0
Process 6	3.8	0.6	0.4	0.6	1.0	1.8	0.6	0.2	0.6	1.0
Process 7	1.3	1.0	0.5	0.5	1.0	0.3	1.0	0.2	0.5	1.0
Process 8	0.5	0.5	0.6	0.2	0.2	0.2	0.2	0.1	0.9	1.0
Process 9	1.5	1.2	0.8	1.0	1.0	1.5	0.2	0.2	1.0	0.9
Process 10	0.9	0.5	0.4	1.2	1.0	0.9	0.5	0.1	1.2	0.8
Process 11	1.7	1.6	1.5	1.8	1.0	1.1	0.6	0.1	1.8	1.0
Process 12	0.6	0.4	0.2	0.4	0.3	0.1	0.4	0.2	0.4	0.6
Process 13	3.0	1.5	1.5	1.6	1.2	0.1	0.5	1.5	1.6	0.4
Process 14	0.5	1.0	0.5	0.2	0.3	0.1	1.0	0.3	0.2	0.2
Process 15	2.0	1.0	1.1	0.4	0.8	1.0	1.0	0.1	0.1	1.0
Process 16	0.8	0.4	0.6	0.7	0.5	0.8	0.4	0.3	0.7	0.5
Process 17	0.8	1.4	1.9	0.8	0.5	0.8	0.4	0.9	0.8	0.2
Process 18	1.9	1.5	2.0	2.0	1.0	0.9	0.5	1.0	1.0	1.0
Process 19	2.5	2.0	2.4	2.2	2.0	2.5	2.0	0.4	2.2	1.0
Process 20	2.4	2.5	2.0	0.8	2.0	0.4	0.5	1.0	0.8	1.0
Process 21	2.4	2.5	1.8	0.9	1.0	0.4	0.5	0.8	0.9	0.4
Process 22	5.8	6.0	5.5	6.0	3.0	0.8	6.0	0.5	2.0	3.0
Process 23	4.0	2.5	2.0	2.0	3.0	2.0	0.5	1.0	1.0	1.0
Process 24	3.0	3.2	3.1	3.1	2.0	2.0	2.2	0.1	1.1	2.0
Process 25	2.5	2.0	1.8	1.8	2.0	1.5	2.0	0.2	1.8	1.0
Process 26	1.5	1.0	0.5	0.5	1.0	0.5	1.0	0.5	0.5	1.0
Process 27	0.8	0.4	0.2	0.4	0.2	0.8	0.4	0.1	0.4	0.5
Process 28	2.0	0.7	0.9	0.8	1.0	0.2	0.1	0.1	0.1	0.1
Process 29	0.9	1.9	1.8	0.9	1.0	0.9	0.9	0.8	0.9	1.0
Process 30	3.0	3.0	2.5	2.2	1.0	1.0	1.0	0.5	0.2	1.0
Process 31	3.9	3.0	2.0	2.1	1.0	0.9	1.0	1.0	1.1	1.0
Process 32	1.5	3.0	2.4	1.0	1.0	0.2	0.3	0.4	2.0	1.0
Process 33	0.9	1.0	5.0	2.5	1.0	0.1	1.0	1.0	2.5	1.0
Process 34	1.6	1.5	0.9	0.9	1.0	0.1	0.1	0.1	0.1	1.0
Process 35	1.7	2.0	1.0	1.0	2.0	0.2	0.1	0.1	1.0	1.0
Process 36	4.3	3.0	1.0	1.1	2.0	0.1	0.2	1.0	1.1	1.0
Process 37	6.8	6.5	6.0	6.2	5.0	0.8	0.5	2.0	0.2	1.0
Process 38	0.9	0.5	0.3	0.4	0.8	0.1	0.5	0.3	0.4	1.0

Table D4. Purchase prices (10² \$/t) for chemicals in case study 2.

Chemicals	Period 1	Period 2	Period 3	Period 4	Period 5	Period 6	Period 7	Period 8	Period 9	Period 10
A	8.2	9.0	5.5	8.0	8.0	8.2	9.0	5.5	8.0	8.0
B	4.0	3.3	4.2	4.0	4.0	4.0	3.3	4.2	4.0	4.0
C	4.4	5.5	3.0	2.0	3.0	4.4	5.5	3.0	2.0	3.0
D	3.5	3.3	3.2	3.1	3.2	3.5	3.3	3.2	3.1	3.2
E	8.6	8.8	8.0	7.5	8.0	8.6	8.8	8.0	7.5	8.0
F	5.5	6.0	6.2	5.0	6.2	5.5	6.0	6.2	5.0	6.2
G	0.4	0.3	1.0	1.1	0.8	0.4	0.3	1.0	1.1	0.8
H	6.6	6.1	7.0	5.0	6.0	6.6	6.1	7.0	5.0	6.0
I	4.1	5.2	5.8	4.0	5.0	4.1	5.2	5.8	4.0	5.0
J	2.6	2.5	3.0	2.2	2.5	2.6	2.5	3.0	2.2	2.5
K	0.0	0.0	0.0	0.0	0.0	0.0	0.0	0.0	0.0	0.0
L	0.0	0.0	0.0	0.0	0.0	0.0	0.0	0.0	0.0	0.0
M	0.0	0.0	0.0	0.0	0.0	0.0	0.0	0.0	0.0	0.0
N	0.0	0.0	0.0	0.0	0.0	0.0	0.0	0.0	0.0	0.0
O	0.0	0.0	0.0	0.0	0.0	0.0	0.0	0.0	0.0	0.0
P	0.0	0.0	0.0	0.0	0.0	0.0	0.0	0.0	0.0	0.0
Q	0.0	0.0	0.0	0.0	0.0	0.0	0.0	0.0	0.0	0.0
R	0.0	0.0	0.0	0.0	0.0	0.0	0.0	0.0	0.0	0.0
S	0.0	0.0	0.0	0.0	0.0	0.0	0.0	0.0	0.0	0.0
T	0.0	0.0	0.0	0.0	0.0	0.0	0.0	0.0	0.0	0.0
U	0.0	0.0	0.0	0.0	0.0	0.0	0.0	0.0	0.0	0.0
V	0.0	0.0	0.0	0.0	0.0	0.0	0.0	0.0	0.0	0.0
W	0.0	0.0	0.0	0.0	0.0	0.0	0.0	0.0	0.0	0.0
X	0.0	0.0	0.0	0.0	0.0	0.0	0.0	0.0	0.0	0.0
Y	0.0	0.0	0.0	0.0	0.0	0.0	0.0	0.0	0.0	0.0
Z	0.0	0.0	0.0	0.0	0.0	0.0	0.0	0.0	0.0	0.0
AA	0.0	0.0	0.0	0.0	0.0	0.0	0.0	0.0	0.0	0.0
AB	0.0	0.0	0.0	0.0	0.0	0.0	0.0	0.0	0.0	0.0

Table D5. Sale prices (10² \$/t) for chemicals in case study 2.

Chemicals	Period 1	Period 2	Period 3	Period 4	Period 5	Period 6	Period 7	Period 8	Period 9	Period 10
A	0.0	0.0	0.0	0.0	0.0	0.0	0.0	0.0	0.0	0.0
B	0.0	0.0	0.0	0.0	0.0	0.0	0.0	0.0	0.0	0.0
C	0.0	0.0	0.0	0.0	0.0	0.0	0.0	0.0	0.0	0.0
D	0.0	0.0	0.0	0.0	0.0	0.0	0.0	0.0	0.0	0.0
E	0.0	0.0	0.0	0.0	0.0	0.0	0.0	0.0	0.0	0.0
F	0.0	0.0	0.0	0.0	0.0	0.0	0.0	0.0	0.0	0.0
G	0.0	0.0	0.0	0.0	0.0	0.0	0.0	0.0	0.0	0.0
H	0.0	0.0	0.0	0.0	0.0	0.0	0.0	0.0	0.0	0.0
I	0.0	0.0	0.0	0.0	0.0	0.0	0.0	0.0	0.0	0.0
J	0.0	0.0	0.0	0.0	0.0	0.0	0.0	0.0	0.0	0.0
K	8.4	9.9	8.0	7.5	7.5	8.4	9.9	8.0	7.5	7.5
L	6.3	7.0	6.5	6.4	6.4	6.3	7.0	6.5	6.4	6.4
M	6.4	7.2	7.0	8.6	7.0	6.4	7.2	7.0	8.6	7.0
N	5.5	5.4	3.0	2.5	4.5	5.5	5.4	3.0	2.5	4.5
O	5.4	4.0	3.5	3.3	4.5	5.4	4.0	3.5	3.3	4.5
P	12.8	12.0	11.0	10.0	10.0	12.8	12.0	11.0	10.0	10.0
Q	7.3	5.0	4.0	3.3	4.0	7.3	5.0	4.0	3.3	4.0
R	7.5	6.0	5.0	4.5	4.5	7.5	6.0	5.0	4.5	4.5
S	6.1	7.5	7.0	6.2	7.2	6.1	7.5	7.0	6.2	7.2
T	5.4	5.0	8.0	8.2	6.4	5.4	5.0	8.0	8.2	6.4
U	7.4	7.0	4.0	4.1	5.6	7.4	7.0	4.0	4.1	5.6
V	7.9	3.0	3.2	3.1	4.5	7.9	3.0	3.2	3.1	4.5
W	3.1	2.0	1.8	1.0	1.2	3.1	2.0	1.8	1.0	1.2
X	7.5	8.0	7.5	9.0	7.8	7.5	8.0	7.5	9.0	7.8
Y	1.6	1.4	1.3	1.3	1.5	1.6	1.4	1.3	1.3	1.5
Z	3.3	4.0	4.1	1.5	3.8	3.3	4.0	4.1	1.5	3.8
AA	0.0	0.0	0.0	0.0	0.0	0.0	0.0	0.0	0.0	0.0
AB	0.0	0.0	0.0	0.0	0.0	0.0	0.0	0.0	0.0	0.0

Table D6. Operating costs (10² \$/t) for processes in case study 2.

Process	Period 1	Period 2	Period 3	Period 4	Period 5	Period 6	Period 7	Period 8	Period 9	Period 10
Process 1	0.8	0.5	0.4	0.6	0.6	0.8	0.5	0.4	0.6	0.6
Process 2	1.5	1.6	1.5	2.0	2.0	1.5	1.6	1.5	2.0	2.0
Process 3	1.0	1.2	1.0	1.8	1.8	1.0	1.2	1.0	1.8	1.8
Process 4	1.1	1.0	0.8	1.8	1.8	1.1	1.0	0.8	1.8	1.8
Process 5	1.1	0.8	0.6	0.5	0.5	1.1	0.8	0.6	0.5	0.5
Process 6	0.7	0.5	0.6	0.9	0.9	0.7	0.5	0.6	0.9	0.9
Process 7	1.0	0.7	0.5	0.9	0.9	1.0	0.7	0.5	0.9	0.9
Process 8	2.5	2.0	1.8	2.0	2.0	2.5	2.0	1.8	2.0	2.0
Process 9	1.5	1.5	1.4	1.0	1.0	1.5	1.5	1.4	1.0	1.0
Process 10	2.0	1.8	1.6	0.5	1.6	2.0	1.8	1.6	0.5	1.6
Process 11	2.0	1.8	1.8	0.9	1.8	2.0	1.8	1.8	0.9	1.8
Process 12	0.7	0.5	0.4	0.4	0.5	0.7	0.5	0.4	0.4	0.5
Process 13	0.7	0.6	0.6	0.6	0.6	0.7	0.6	0.6	0.6	0.6
Process 14	2.0	2.0	1.8	0.9	1.8	0.01	0.01	1.8	0.9	1.8
Process 15	1.6	1.5	1.4	1.5	1.5	0.6	1.5	1.4	1.5	1.5
Process 16	1.0	1.2	1.0	1.2	1.2	1.0	1.2	1.0	1.2	1.2
Process 17	1.3	1.0	0.9	0.1	1.0	1.3	1.0	0.9	0.1	1.0
Process 18	0.8	0.4	0.2	0.2	0.4	0.8	0.4	0.2	0.2	0.4
Process 19	1.5	1.0	1.1	1.0	1.0	1.5	1.0	1.1	1.0	1.0
Process 20	2.5	2.0	2.1	2.2	2.1	2.5	2.0	2.1	2.2	2.1
Process 21	3.0	3.0	2.7	2.8	2.8	3.0	3.0	2.7	2.8	2.8
Process 22	1.5	1.2	1.0	0.9	0.9	1.5	1.2	1.0	0.9	0.9
Process 23	1.3	1.0	0.8	0.1	0.8	1.3	1.0	0.8	0.1	0.8
Process 24	2.0	1.5	1.4	1.0	1.0	2.0	1.5	1.4	1.0	1.0
Process 25	2.3	2.0	1.8	1.9	1.8	2.3	2.0	1.8	1.9	1.8
Process 26	1.0	1.1	1.0	0.9	1.0	1.0	1.1	1.0	0.9	1.0
Process 27	1.5	1.0	0.8	0.6	0.8	1.5	1.0	0.8	0.6	0.8
Process 28	1.0	0.8	0.7	0.7	0.7	1.0	0.8	0.7	0.7	0.7
Process 29	2.0	1.8	1.9	1.9	1.6	2.0	1.8	1.9	1.9	1.6
Process 30	2.0	1.9	1.7	1.6	1.6	2.0	1.9	1.7	1.6	1.6
Process 31	3.0	2.5	2.0	1.6	1.0	3.0	2.5	2.0	1.6	1.0
Process 32	2.0	1.9	2.0	1.0	1.0	2.0	1.9	2.0	1.0	1.0
Process 33	3.0	3.1	3.2	3.1	3.1	3.0	3.1	3.2	3.1	3.1
Process 34	0.4	0.3	0.2	0.4	0.4	0.4	0.3	0.2	0.4	0.4
Process 35	1.3	1.2	1.1	0.1	1.1	1.3	1.2	1.1	0.1	1.1
Process 36	3.0	2.8	2.4	2.2	2.2	3.0	2.8	2.4	2.2	2.2
Process 37	3.5	3.0	2.5	3.0	3.0	3.5	3.0	2.5	3.0	3.0
Process 38	1.0	1.2	1.0	1.1	1.1	1.0	1.2	1.0	1.1	1.1

Notation

DDSRO Framework

The main notations used in the DDSRO modeling framework are listed below.

b	vector of objective coefficients corresponding to second-stage decisions
c	vector of objective coefficients corresponding to first-stage decisions
u	vector of uncertainties
x	vector of first-stage decisions
y_s	vector of second-stage decisions for data class <i>s</i>
C	total number of data classes in uncertainty data
m(<i>s</i>)	total number of basic uncertainty sets for data class <i>s</i>
M	truncation level in the Variational inference
M₀	constant with a very large value
U_s	uncertainty set for data class <i>s</i>
s	index of data class
Λ_i	scaling factor in the data-driven uncertainty set
τ_i	a hyper-parameter for Beta distribution in the Variational inference
ν_i	a hyper-parameter for Beta distribution in the Variational inference
γ_i	weight of mixture component
γ*	threshold value for the weight of mixture component
Φ_{s,i}	uncertainty budget in data-driven uncertainty set
A	coefficient matrix corresponding to the first-stage decisions
M	coefficient matrix corresponding to the uncertainties
T	technology matrix in the DDSRO framework
W	recourse matrix in the DDSRO framework

Application to planning of process networks

The sets, parameters, and variables used in the application part are summarized below. Note that all parameters are denoted in lower-case symbols, and all variables are denoted in upper-case symbols.

Sets/indices

I	set of processes indexed by i
J	set of chemicals indexed by j
T	set of time periods indexed by t
Ξ	set of data classes indexed by s

Parameters

ce_i	maximum number of expansions for process i over the planning horizon
du_{jt}	demand of chemical j in time period t
su_{jt}	supply of chemical j in time period t
$c1_{it}$	variable investment cost for process i in time period t
$c2_{it}$	fixed investment cost for process i in time period t
$c3_{it}$	unit operating cost for process i in time period t
$c4_{it}$	purchase price of chemical j in time period t
cb_t	maximum allowable investment in time period t
qe_{it}^L	lower bound for capacity expansion of process i in time period t
qe_{it}^U	upper bound for capacity expansion of process i in time period t
v_{jt}	sale price of chemical j in time period t
κ_{ij}	mass balance coefficient for chemical j in process i

Binary variables

Y_{it}	binary variable that indicates whether process i is chosen for expansion in time period t
----------	---

Continuous variables

P_{sjt}	purchase amount of chemical j in time period t for data class s
Q_{it}	total capacity of process i in time period t
QE_{it}	capacity expansion of process i in time period t

SA_{sjt}	sale amount of chemical j in time period t for data class s
W_{sit}	operation level of process i in time period t for data class s

Literature Cited

- [1] S. J. Qin, "Survey on data-driven industrial process monitoring and diagnosis," *Annual Reviews in Control*, vol. 36, pp. 220-234, 2012.
- [2] A. Karpathy, G. Toderici, S. Shetty, T. Leung, R. Sukthankar, and L. Fei-Fei, "Large-scale video classification with convolutional neural networks," in *2014 IEEE Conference on Computer Vision and Pattern Recognition*, 2014, pp. 1725-1732.
- [3] X. Tong, X. Tian, Y. Yi, H. Chang, and W. Xiaogang, "Learning from massive noisy labeled data for image classification," in *2015 IEEE Conference on Computer Vision and Pattern Recognition*, 2015, pp. 2691-2699.
- [4] M. I. Jordan and T. M. Mitchell, "Machine learning: Trends, perspectives, and prospects," *Science*, vol. 349, pp. 255-260, 2015.
- [5] K. P. Murphy, *Machine learning: A probabilistic perspective*: MIT press, 2012.
- [6] M. S. Afzal, W. Tan, and T. Chen, "Process monitoring for multimodal processes with mode-reachability constraints," *IEEE Transactions on Industrial Electronics*, vol. 64, pp. 4325-4335, 2017.
- [7] F. Sebastiani, "Machine learning in automated text categorization," *ACM Comput. Surv.*, vol. 34, pp. 1-47, 2002.
- [8] B. A. Calfa, I. E. Grossmann, A. Agarwal, S. J. Bury, and J. M. Wassick, "Data-driven individual and joint chance-constrained optimization via kernel smoothing," *Computers & Chemical Engineering*, vol. 78, pp. 51-69, 2015.
- [9] C. Ning and F. You, "Data-driven adaptive nested robust optimization: General modeling framework and efficient computational algorithm for decision making under uncertainty," *AIChE Journal*, vol. 63, pp. 3790-3817, 2017.
- [10] R. Jiang and Y. Guan, "Data-driven chance constrained stochastic program," *Mathematical Programming*, vol. 158, pp. 291-327, 2016.
- [11] C. Shang, X. Huang, and F. You, "Data-driven robust optimization based on kernel learning," *Computers & Chemical Engineering*, vol. 106, pp. 464-479, 2017.
- [12] C. Ning and F. You, "A data-driven multistage adaptive robust optimization framework for planning and scheduling under uncertainty," *AIChE Journal*, vol. 63, pp. 4343-4369, 2017.
- [13] D. Bertsimas, V. Gupta, and N. Kallus, "Data-driven robust optimization," *Mathematical Programming*, pp. 1-58, 2017.
- [14] D. Bertsimas and N. Kallus, "From predictive to prescriptive analytics," *arXiv preprint arXiv:1402.5481*, 2014.
- [15] N. V. Sahinidis, "Optimization under uncertainty: State-of-the-art and opportunities," *Computers & Chemical Engineering*, vol. 28, pp. 971-983, 2004.
- [16] I. E. Grossmann, R. M. Apap, B. A. Calfa, P. García-Herreros, and Q. Zhang, "Recent advances in mathematical programming techniques for the optimization of process systems under uncertainty," *Computers & Chemical Engineering*, vol. 91, pp. 3-14, 2016.
- [17] E. N. Pistikopoulos, "Uncertainty in process design and operations," *Computers & Chemical Engineering*, vol. 19, pp. 553-563, 1995.

- [18] J. M. Mulvey, R. J. Vanderbei, and S. A. Zenios, "Robust optimization of large-scale systems," *Operations Research*, vol. 43, pp. 264-281, 1995.
- [19] A. Ben-Tal and A. Nemirovski, "Robust optimization – methodology and applications," *Mathematical Programming*, vol. 92, pp. 453-480, 2002.
- [20] J. R. Birge and F. Louveaux, *Introduction to stochastic programming*: Springer Science & Business Media, 2011.
- [21] V. Gabrel, C. Murat, and A. Thiele, "Recent advances in robust optimization: An overview," *European Journal of Operational Research*, vol. 235, pp. 471-483, 2014.
- [22] D. Bertsimas, D. B. Brown, and C. Caramanis, "Theory and applications of robust optimization," *SIAM Review*, vol. 53, pp. 464-501, 2011.
- [23] J. Gong, D. J. Garcia, and F. You, "Unraveling optimal biomass processing routes from bioconversion product and process networks under uncertainty: An adaptive robust optimization approach," *ACS Sustainable Chemistry & Engineering*, vol. 4, pp. 3160-3173, 2016.
- [24] J. Gong and F. You, "Optimal processing network design under uncertainty for producing fuels and value-added bioproducts from microalgae: Two-stage adaptive robust mixed integer fractional programming model and computationally efficient solution algorithm," *AIChE Journal*, vol. 63, pp. 582-600, 2017.
- [25] H. Shi and F. You, "A computational framework and solution algorithms for two-stage adaptive robust scheduling of batch manufacturing processes under uncertainty," *AIChE Journal*, vol. 62, pp. 687-703, 2016.
- [26] J. Gao and F. You, "Deciphering and handling uncertainty in shale gas supply chain design and optimization: Novel modeling framework and computationally efficient solution algorithm," *AIChE Journal*, vol. 61, pp. 3739-3755, 2015.
- [27] Y. Chu and F. You, "Integration of scheduling and dynamic optimization of batch processes under uncertainty: Two-stage stochastic programming approach and enhanced generalized benders decomposition algorithm," *Industrial & Engineering Chemistry Research*, vol. 52, pp. 16851-16869, 2013.
- [28] H. Kasivisvanathan, A. T. Ubando, D. K. S. Ng, and R. R. Tan, "Robust optimization for process synthesis and design of multifunctional energy systems with uncertainties," *Industrial & Engineering Chemistry Research*, vol. 53, pp. 3196-3209, 2014.
- [29] S. R. Cardoso, A. P. F. D. Barbosa-Póvoa, and S. Relvas, "Design and planning of supply chains with integration of reverse logistics activities under demand uncertainty," *European Journal of Operational Research*, vol. 226, pp. 436-451, 2013.
- [30] S. Liu, S. S. Farid, and L. G. Papageorgiou, "Integrated optimization of upstream and downstream processing in biopharmaceutical manufacturing under uncertainty: A chance constrained programming approach," *Industrial & Engineering Chemistry Research*, vol. 55, pp. 4599-4612, 2016.
- [31] J. R. Birge, "State-of-the-art-survey—stochastic programming: Computation and applications," *INFORMS Journal on Computing*, vol. 9, pp. 111-133, 1997.
- [32] A. Bonfill, A. Espuña, and L. Puigjaner, "Addressing robustness in scheduling batch processes with uncertain operation times," *Industrial & Engineering Chemistry Research*, vol. 44, pp. 1524-1534, 2005.
- [33] A. Bonfill, M. Bagajewicz, A. Espuña, and L. Puigjaner, "Risk management in the scheduling of batch plants under uncertain market demand," *Industrial & Engineering Chemistry Research*, vol. 43, pp. 741-750, 2004.

- [34] P. Liu, E. N. Pistikopoulos, and Z. Li, "Decomposition based stochastic programming approach for polygeneration energy systems design under uncertainty," *Industrial & Engineering Chemistry Research*, vol. 49, pp. 3295-3305, 2010.
- [35] B. H. Gebreslassie, Y. Yao, and F. You, "Design under uncertainty of hydrocarbon biorefinery supply chains: Multiobjective stochastic programming models, decomposition algorithm, and a comparison between cvar and downside risk," *AIChE Journal*, vol. 58, pp. 2155-2179, 2012.
- [36] L. J. Zeballos, C. A. Méndez, and A. P. Barbosa-Povoa, "Design and planning of closed-loop supply chains: A risk-averse multistage stochastic approach," *Industrial & Engineering Chemistry Research*, vol. 55, pp. 6236-6249, 2016.
- [37] Y. Yuan, Z. Li, and B. Huang, "Robust optimization under correlated uncertainty: Formulations and computational study," *Computers & Chemical Engineering*, vol. 85, pp. 58-71, 2016.
- [38] A. Ben-Tal and A. Nemirovski, "Robust solutions of linear programming problems contaminated with uncertain data," *Math. Programming*, vol. 88, p. 411, 2000.
- [39] D. Bertsimas and M. Sim, "The price of robustness," *Oper. Res.*, vol. 52, p. 35, 2004.
- [40] A. Ben-Tal, L. E. Ghaoui, and A. Nemirovski, *Robust optimization*: Princeton University Press, 2009.
- [41] Z. Li, R. Ding, and C. A. Floudas, "A comparative theoretical and computational study on robust counterpart optimization: I. Robust linear optimization and robust mixed integer linear optimization," *Industrial & Engineering Chemistry Research*, vol. 50, pp. 10567-10603, 2011.
- [42] K. McLean and X. Li, "Robust scenario formulations for strategic supply chain optimization under uncertainty," *Industrial & Engineering Chemistry Research*, vol. 52, pp. 5721-5734, 2013.
- [43] D. Yue and F. You, "Optimal supply chain design and operations under multi-scale uncertainties: Nested stochastic robust optimization modeling framework and solution algorithm," *AIChE Journal*, vol. 62, pp. 3041-3055, 2016.
- [44] C. Liu, C. Lee, H. Chen, and S. Mehrotra, "Stochastic robust mathematical programming model for power system optimization," *IEEE Transactions on Power Systems*, vol. 31, pp. 821-822, 2016.
- [45] F. You and I. E. Grossmann, "Multicut benders decomposition algorithm for process supply chain planning under uncertainty," *Annals of Operations Research*, vol. 210, pp. 191-211, 2013.
- [46] J. Shi, W. J. Lee, Y. Liu, Y. Yang, and P. Wang, "Forecasting power output of photovoltaic systems based on weather classification and support vector machines," *IEEE Transactions on Industry Applications*, vol. 48, pp. 1064-1069, 2012.
- [47] L. Wasserman, *All of statistics: A concise course in statistical inference*: Springer Science & Business Media, 2013.
- [48] T. Campbell and J. P. How, "Bayesian nonparametric set construction for robust optimization," in *2015 American Control Conference (ACC)*, 2015, pp. 4216-4221.
- [49] D. M. Blei and M. I. Jordan, "Variational inference for dirichlet process mixtures," *Bayesian analysis*, vol. 1, pp. 121-143, 2006.
- [50] A. Billionnet, M.-C. Costa, and P.-L. Poirion, "2-stage robust milp with continuous recourse variables," *Discrete Applied Mathematics*, vol. 170, pp. 21-32, 2014.

- [51] B. Zeng and L. Zhao, "Solving two-stage robust optimization problems using a column-and-constraint generation method," *Operations Research Letters*, vol. 41, pp. 457-461, 2013.
- [52] N. V. Sahinidis, I. E. Grossmann, R. E. Fornari, and M. Chathrathi, "Optimization model for long range planning in the chemical industry," *Computers & Chemical Engineering*, vol. 13, pp. 1049-1063, 1989.
- [53] F. You and I. E. Grossmann, "Stochastic inventory management for tactical process planning under uncertainties: Minlp models and algorithms," *AIChE Journal*, vol. 57, pp. 1250-1277, 2011.
- [54] D. Yue and F. You, "Planning and scheduling of flexible process networks under uncertainty with stochastic inventory: Minlp models and algorithm," *AIChE Journal*, vol. 59, pp. 1511-1532, 2013.
- [55] M. L. Liu and N. V. Sahinidis, "Optimization in process planning under uncertainty," *Industrial & Engineering Chemistry Research*, vol. 35, pp. 4154-4165, 1996.
- [56] S. Ahmed and N. V. Sahinidis, "Robust process planning under uncertainty," *Industrial & Engineering Chemistry Research*, vol. 37, pp. 1883-1892, 1998.
- [57] E. Rosenthal, *Gams-a user's guide*. Washington, DC: GAMS Development Corporation, 2008.
- [58] T. S. Ferguson, "A bayesian analysis of some nonparametric problems," *The annals of statistics*, pp. 209-230, 1973.
- [59] J. Sethuraman, "A constructive definition of dirichlet priors," *Statistica Sinica*, vol. 4, pp. 639-650, 1994.
- [60] A. Takeda, S. Taguchi, and R. H. Tütüncü, "Adjustable robust optimization models for a nonlinear two-period system," *Journal of Optimization Theory and Applications*, vol. 136, pp. 275-295, 2008.
- [61] D. Bertsimas, E. Litvinov, X. A. Sun, J. Zhao, and T. Zheng, "Adaptive robust optimization for the security constrained unit commitment problem," *IEEE Transactions on Power Systems*, vol. 28, pp. 52-63, 2013.
- [62] A. Thiele, T. Terry, and M. Epelman, "Robust linear optimization with recourse," *Rapport technique*, pp. 4-37, 2009.
- [63] F. Glover, "Improved linear integer programming formulations of nonlinear integer problems," *Management Science*, vol. 22, pp. 455-460, 1975.